UNIVERSITÉ DU QUÉBEC

MÉMOIRE PRÉSENTÉ À
L'UNIVERSITÉ DU QUÉBEC À TROIS-RIVIÈRES

COMME EXIGENCE PARTIELLE
DE LA MAÎTRISE EN SCIENCES DE L'ENVIRONNEMENT

PAR
SAIDA NEMRI

APPLICATION D'UN MODÈLE HYDROLOGIQUE CONCEPTUEL POUR L'ÉTUDE DES CRUES PRINTANIÈRES AU QUÉBEC

MARS 2019

REMERCIEMENTS

À l'issue de ce travail, je tiens à remercier et à exprimer toute ma gratitude à mon directeur de maîtrise M. Christophe Kinnard, professeur du Département des sciences de l'environnement de l'Université du Québec à Trois-Rivières, de m'avoir donné l'opportunité, pour la confiance qu'il m'a accordée, pour sa disponibilité, son efficacité et l'effort fourni.

Je tiens aussi à remercier les membres du jury qui ont accepté d'évaluer mon travail : MM. Ali Assani et Stéphane Campeau, professeurs du Département des sciences de l'environnement de l'Université du Québec à Trois-Rivières.

Je remercie également chaleureusement mes collègues et amis du Laboratoire en environnement des régions froides (GLACIOLAB), Lisane Arsenault, Okan Aygun, Hadi Mohammadzadeh Khani, Olivier Larouche, Arthur de Grandpré, Matthieu Loyer, Vasana Dharmadasa pour leur écoute, encouragement et tous les agréables moments qu'on a vécu ensemble.

À mes chers parents qui ont toujours été à mes côtés, à mon cher mari que rien n'aurait été possible sans vous et je vous en suis très reconnaissante!

RÉSUMÉ

La problématique envisagée par les hydrologues, dans un contexte de prédominance de neige en hiver et de fonte rapide au printemps, est d'avoir une estimation réaliste du couvert nival et de comprendre la complexité des facteurs qui contrôlent la génération des crues printanières. La modélisation hydrologique et de l'accumulation et la fonte de la neige par des modèles hydrologiques à différentes complexités constituent un outil pour la prévision opérationnelle des crues et la simulation du manteau nival. Dans cette étude, nous chercherons à améliorer la calibration d'un modèle hydrologique conceptuel couplé avec un module de fonte de la neige par l'ajout des données observées de l'équivalent en eau de la neige (ÉEN) dans le but d'obtenir une simulation réaliste du couvert nival dans une première étape. Dans une deuxième étape, nous avons essayé de comprendre la variabilité interannuelle de la magnitude et de la date d'occurrence des pics de crues printanières et de répondre à la question : est-ce que cette variabilité dépend principalement du stock de neige maximal accumulé, et quel est l'effet de la quantité et de l'intensité de la pluie durant la période de fonte sur le pic de crue? La performance de deux modèles, GR4J et Cemaneige, a été testée tout d'abord sur 12 bassins à régime hydrologique naturel et la calibration a été réalisée selon quatre stratégies. Un calage classique par rapport aux débits mesurés a été réalisé en premier temps en utilisant une méthode d'optimisation locale et ensuite avec un algorithme global (SCE-UA) dans la deuxième méthode. La troisième méthode consiste à calibrer indépendamment le module de neige avec l'équivalent en eau (ÉEN) observé aux stations du réseau nivométrique et l'introduire par la suite dans le modèle hydrologique. Une calibration multi-objectif a été entreprise par la suite, où les paramètres du modèle ont été calés par rapport à l'ÉEN et le débit observé, en utilisant un algorithme d'optimisation multi-objectif AMALGAM. Une amélioration de la simulation du couvert nival et du débit par la méthode multi-objectif a été démontrée. Les jeux de paramètres équifinaux ont montré une interaction et une compensation entre les paramètres qui constituent une grande source d'équifinalité. Sur une période de pré-conditionnement des crues, les facteurs liés à la fonte de neige, la pluie liquide enregistrée et l'humidité de sol ont été calculés et par la suite leurs capacités à expliquer les caractéristiques des pics printaniers (magnitude et date d'occurrence) ont été évaluées par une régression linéaire multiple. Nos résultats de régression linéaire démontrent que la variabilité interannuelle de la magnitude de crues printanières à travers les douze bassins dépend des facteurs suivants en ordre d'importance : l'intensité de fonte (moyenne et maximale), le total de la fonte, le total de la pluie, le pic de l'équivalent en eau (ÉEN) et l'humidité du sol. La pluie pré-crue contrôle principalement la variabilité interannuelle du pic de crue dans les bassins forestiers situés plus au nord avec un régime nival. Cependant, l'importance du stock de neige accumulé en hiver contrôle davantage cette variabilité dans les bassins du sud, plus agricoles et à régime davantage pluvio-nival. La date d'occurrence est plutôt expliquée par la pluie pré-crue.

Mots-clés : crues printanières, variabilité interannuelle, magnitude, date d'occurrence, calibration, modèles hydrologiques conceptuels, ÉEN, incertitude des paramètres, changements climatiques.

TABLE DES MATIÈRES

CHAPITRE I

INTRODUCTION

1.1 Mise en contexte

L'hydrologie dans les pays nordiques comme le Canada se distingue par de longs hivers dominés par la neige et une fonte printanière rapide. Cette fonte saisonnière fournit plus de 80 % du ruissellement annuel dans les prairies canadiennes (Buttle, 2016). Au Québec la quantité de neige accumulée est très importante avec un maximum annuel moyen de 200 à 300 mm d'équivalent en eau (Brown, 2010). Dans le nord du Québec, l'accumulation de neige commence en octobre et continue jusqu'au mois de mai tandis qu'au sud la neige commence à s'accumuler en novembre jusqu'à la fonte en mars-avril (Buttle et al., 2016). Le régime de ruissellement est fortement influencé par l'écoulement de la fonte des neiges au printemps et le débit le plus élevé est typiquement mesuré pendant cette période, le régime hydrologique des rivières se caractérise alors par une principale crue printanière (Adamowski, 2000), une crue secondaire faible liée aux précipitations en automne, une période de faible débit en hiver résultant de la chute de précipitations sous forme de neige et une autre période de faible débit en été suite à la diminution des précipitations liquides et solides (Assani et al., 2012). La relation entre le volume de neige et les débits de crues printanières a constitué le sujet de recherche de plusieurs études dans le but de prédire les crues, étudier les facteurs qui les préconditionnent et estimer la contribution du volume de la fonte à ces débits. Pour les gestionnaires des ressources en eau, une connaissance précise de l'équivalent en eau des neiges (ÉEN) des manteaux nival dans les derniers jours d'hiver est très importante pour la prévision du moment et du volume de crue printanière (Turcotte et al., 2010). L'état hydrique du sol ainsi que la contribution de la pluie aux crues peuvent influencer l'estimation de la vraie contribution nivale à ces crues. La modélisation de l'accumulation et la fonte de la neige par des modèles de neige et hydrologiques à différentes complexités constituent un outil pour la prévision opérationnelle des crues.

Une simulation réaliste du manteau nival présent sur le bassin suivi d'une bonne calibration et validation de ces modèles hydrologiques peut fournir une estimation réaliste de la contribution respective de la pluie et de la fonte de la neige aux débits en réponse aux conditions hydro-climatiques au moment des crues.

1.2 Problématique

Les crues printanières causent parfois des inondations qui provoquent d'importants dégâts matériels. Une meilleure compréhension des conditions hydroclimatiques causant les crues est souhaitable et représente la première étape vers le développement de méthodes de prévision des crues à l'échelle opérationnelle (jours) et saisonnière (mois). L'étude des facteurs préconditionnant les crues est difficile au Québec en raison du peu de données hydrométéorologiques disponibles. Quoique des données fiables de précipitation et températures existent, le bilan d'humidité du sol et la quantité de neige au sol, deux facteurs influençant fortement les crues, ne sont pas mesurés de façon routinière. L'utilisation de modèles hydrologiques peut ainsi contribuer à améliorer notre compréhension des facteurs qui préconditionnent les crues printanières. La calibration classique des paramètres des modèles de neige se fait typiquement par rapport aux débits avec des critères de performance globale calculés à partir des débits observés et simulés (Troin et al., 2015; Valéry et al., 2014a, 2014b). Sauf que dans un bassin dominé par la fonte des neiges, une bonne simulation de débit à la sortie ne garantit pas toujours une bonne représentation des processus de neige.

1.3 Objectifs

L'objectif principal de ce projet de recherche est d'étudier les caractéristiques hydrométéorologiques des crues printanières au Québec à l'aide d'un modèle hydrologique simplifié (modèle GR4J) et un modèle de fonte à base de degré/jours (modèle Cemaneige) pour la compréhension des facteurs qui préconditionnent les crues printanières au Québec. Les objectifs spécifiques suivants ont été poursuivis :

1) Tester la performance d'un modèle pluie-neige-débit pour 12 bassins au Québec. La question principale qui sous-tend cet objectif est la suivante : un modèle conceptuel et parcimonieux est-il adéquat pour bien simuler l'évolution du couvert nival et les débits de crues printanières? Le choix de la stratégie de calage/validation des deux modèles est le premier défi à relever dans cette étape, qui comprend le choix de la fonction objectif et d'un algorithme d'optimisation permettant d'utiliser simultanément les relevés de neige et les débits observés. Nos principales hypothèses qui ont été testées pour cette partie sont 1) la calibration multi-objectif (débit et neige) améliore la simulation des débits et du manteau nival et augmente la stabilité des paramètres (réduit l'équifinalité); 2) les paramètres hydrologiques seront spatialement plus homogènes, et mieux reliés aux caractéristiques du bassin lorsque les paramètres neige sont prescrits. Cet objectif va être l'objet du chapitre I.

2) Identifier les variables, telles que simulées par le modèle GR4J-Cemaneige, qui préconditionnent les crues (apports de la fonte de la neige, pluies, bilan d'humidité du sol) et leurs variations spatiales. La question qui sous-tend cet objectif est la suivante : quelle est la contribution respective de la pluie, de la fonte des neiges et de l'état hydrique du sol aux pics de crues printanières? Les hypothèses qui ont été testées sont 1) la contribution de la pluie au volume de crue printanière varie entre les bassins, selon la latitude; 2) la variabilité interannuelle de la magnitude du pic de crue printanière ainsi que sa date d'occurrence dépend principalement du stock de neige accumulé, et secondairement de la quantité de pluie durant la période de fonte; 3) plus le stock de neige est important, plus longue sera la fonte et le niveau des rivières montera plus haut; 4) plus il y a de pluie durant la fonte, plus le niveau montera. Les résultats de cette deuxième partie seront l'objet du chapitre II.

CHAPITRE II

COMPARING CALIBRATION STRATEGIES OF A CONCEPTUAL SNOW HYDROLOGY MODEL AND THEIR IMPACT ON MODEL PERFORMANCE AND PARAMETER IDENTIFIABILITY

Article en attente de soumission au journal scientifique *Journal of Hydrology*

Saida Nemri[1], Christophe Kinnard[1]

[1] Département des Sciences de l'environnement, Université du Québec à Trois-Rivières, C. P. 500, Trois-Rivières, Québec, G9A 5H7 Canada

Corresponding author: Christophe Kinnard

E-mail: Christophe.Kinnard@uqtr.ca

Abstract

Having a realistic estimation of snow cover by conceptual hydrological models continues to challenge hydrologists. The calibration of the free parameters is an unavoidable step in modeling and the uncertainties resulting from the use of this optimal set remains a source of concern, especially in forecasting applications and climate changes impact assessments. The objective of this study is to improve the calibration of the conceptual hydrological model GR4J coupled with the snowmelt model Cemaneige, in order to obtain a more realistic simulation of the snow water equivalent (SWE) and to reduce the uncertainty of the free parameters. The performance of the two models was tested over twelve snow-dominated basins in southern Quebec, Canada. Four calibration strategies were adopted and compared. In the first two strategies, the parameters were calibrated against observed streamflow only using a local and a global algorithm. In the third and fourth strategies the calibration of snow and hydrological parameters was performed against observed discharge and snow water equivalent (SWE) measured at snow survey points, first separately, and then with a multi-objective approach using the AMALGAM algorithm. An ensemble of equifinal parameters was used to compare the capacity of the global and multi-objective algorithms to improve the parameters identifiability, and to quantify their uncertainties in the detection of climate change impact on spring peak streamflow. Results show that the inclusion of snow observations using the multi-objective approach improved the simulation of SWE and the identifiability of the parameters. The large number of equifinal parameters found during calibration shows the importance of structure no-identifiability in the coupled GR4J-Cemaneige model. The uncertainty induced by using the best numerical optimal solution rather than equifinal parameters giving a similar performance, for detecting changes in maximum spring streamflow in response to climate warming in snow-dominated basins, is not negligible.

Keywords: conceptual hydrologic model; calibration; SWE; structural uncertainty; equifinality; climate change.

Introduction

In cold regions, the accumulation of snow in winter and the rapid melting during the warm period is the main source of the high spring streamflow. In these areas, a good estimation of the amount of snow present in a basin before melting is the starting point of any floods forecasting and essential to understand the interannual variability of the magnitude and the timing of snow melting. In the Canadian province of Quebec, the amount of accumulated snow is considerable, with a mean annual maximum of 200 to 300 mm in terms of water equivalent (Brown, 2010). Melting of this snow in the spring represents an important source of freshwater which shapes the ecology of the region as well as hydropower generation capacity (Brown, 2010). In Québec, a network of snow survey measurement sites was installed by the Ministry of Environment and Fight Against Climate Change (MELCC) since 1928 for operational purposes to monitor snow cover depth and snow water equivalent (SWE) (Poirier et al., 2014). Remote sensing data (passive and active microwaves) has also been widely used for estimating SWE but problems remain in forested areas and regions with thick snow cover, as well as in steep mountain terrain (Brown, 2010; Turcotte et al., 2007). Consequently, hydrological models of different complexities have been mainly used by hydrologists to simulate the accumulation and melting of snow and to estimate streamflow for operational purposes (Turcotte et al., 2010). Several rainfall-runoff models have shown a great ability to simulate runoff, but in a snow-dominated basin, a good streamflow simulation does not always guarantee a good representation of the snow processes (Udnæs et al., 2007). Accurate simulations of both river discharge and snow cover are desirable if these models are to be used to project potential impacts of climate change on snow hydrology.

Model calibration is necessary to estimate the free parameters in conceptual models, and many questions still arise about how the uncertainties in the calibrated parameters impact streamflow forecasts as well as model-based climate change projections. In its beginning, the calibration problem was a numerical problem which often led to miscalibration, as described by Andréassian et al. (2012), due to the high-dimensional response surfaces of the parameters and the failure of algorithms to locate global mathematical optima without being trapped by local ones (Moradkhani et al., 2009). Therefore, several optimization algorithms (local, global) were developed during the last decades, with the objective to improve both the search algorithms and the evaluation criteria used during calibration and validation. Several important reviews in the literature have illustrated and compared the optimization methods developed and used by hydrologists (Duan et al., 1992; Efstratiadis et al., 2010; Gupta et al., 2006; Gupta et al., 2003b; Moradkhani et al., 2009). The Shuffled Complex Evolution – University of Arizona (SCE-UA) algorithm elaborated by Duan et al. (1992) is often considered the most efficient for the calibration of conceptual and global hydrological models because of its ability to find global optima (Arsenault et al., 2013). Despite the development of sophisticated automatic algorithms and calibration methods, the uncertainties related to calibrated parameters has persisted while new uncertainty problems have been revealed (Blasone, 2007). The major issue is the multiplicity of optimal parameters, whereas several sets of parameters give the same performance, and this remains at the heart of all studies on the robustness of hydrological models. The concept of a single optimal set has been gradually replaced to accept that a group of parameter sets can give equally satisfying simulations, a concept called 'equifinality' by Beven (2006). Numerous hydrological studies have focused on quantifying equifinality and its impact on simulations (Arsenault, 2015; Arsenault et al., 2014; Beven, 2006; Beven et al., 2001; Foulon et al., 2018). This multiplicity is also explained by the dependence between the optimized parameter values and the climatic conditions of the calibration period, which was highlighted by several authors using a multi-calibration approach on climatically contrasted sub-periods (i.e. periods of similar climatic conditions) (Blasone, 2007; Brigode et al., 2013; Coron et al., 2014; Coron et al., 2012; Merz et al., 2011; Perrin, 2000; Seiller et al., 2012; Vos et al., 2010). These studies also demonstrate the problem of the temporal transferability of parameters, i.e. when they are calibrated over a period and transferred to another period with different climatic conditions. Gupta et al. (1998) also explained this multiplicity of optimal sets by the natural multi-objectivity of the parameters that are related to the calibration objective function. In the context of snow-dominated basins, the parameters of the snow models are most often calibrated simultaneously with the hydrological parameters against observed discharge, without taking into account any information about snow (e.g. Troin et al., 2015; Valéry et al., 2014a, 2014b). Hence in addition to the aforementioned calibration uncertainties, the representativity of key processes such as snow melting represents another important issue in these basins, especially when using these models for climate change studies. A multi-objective approach was recommended by hydrologists to replace this classical calibration method to improve the simulation of all processes and to reduce uncertainties in the free parameters (Efstratiadis et al., 2010; Gupta et al., 1998). This is typically carried out using evolutionary algorithms that search for acceptable trade-offs between objective functions and leads to a feasible vector called 'Pareto optimality' (Yapo et al., 1998). Several studies have already shown the utility of including snow observations in the calibration of different models within a multi-objective approach to improve the simulation of SWE (Duethmann et al., 2014; Fenicia et al., 2007; Finger et al., 2011; Madsen, 2003; Parajka et al., 2008; Parajka et al., 2007; Turcotte et al., 2003). Snow cover area (SCA) estimated by satellite sensors such as MODIS and Landsat are among the snow observations used to calibrate and validate snowmelt models (Duethmann et al., 2014; Finger et al., 2011; Parajka et al., 2008). In Quebec, Roy et al. (2010) incorporated snow-covered area derived from remote sensing to improve spring streamflow simulation with the Hydrotel model. Turcotte et al. (2007) used snow survey observations (density and SWE) to calibrate the Hydrotel model at each snow survey station.

Lumped or semi-distributed models are among the most used models to assess climate change impacts on water resources (Wilby, 2005). Uncertainties in climatic scenarios and downscaling techniques are known to cause significant uncertainties in hydrological impact assessments (e.g. Wilby, 2005). Several recent studies have also focused on the uncertainties induced by hydrological modeling, i.e. those resulting from structural and parameterization errors. Some of these studies attempted to rank these uncertainties, but there is no agreement yet on the ranking of hydrological and climatic errors, and between hydrological uncertainties themselves, i.e. structural errors and parameters equifinality (Bennett et al., 2012; Kay et al., 2009; Seiller et al., 2014; Teng et al., 2011; Wilby, 2005; Wilby et al., 2006). Uncertainty arising from the model structure is typically evaluated by using multiple hydrological models having different structures, and so different representations of hydrology processes, to see the spread of future hydrological projections for the same climatic scenario (e.g. Chen et al., 2011; Jiang et al., 2007; Poulin et al., 2011; Seiller et al., 2014). Seiller et al. (2014) compared the uncertainties arising from climatic variability and the choice between twenty lumped hydrological models and seven snow models, and found that the uncertainty in simulated streamflow arising from models structures was less important than uncertainties in climate scenarios. Wilby et al. (2006) ranked parameter uncertainty as the third most important source, behind the choice of GCM and downscaling technique. Chen et al. (2011) ranked the structural uncertainty as the fourth and parameters uncertainties as the fifth most important, behind climatic uncertainties, for a Canadian catchment. In all these studies, structural and parameterization uncertainties were evaluated jointly. The impacts of parameters non-uniqueness on hydrological projections have been addressed by generating equifinal parameter sets using different methods and running the model using this ensemble. Wilby (2005) studied the uncertainties caused by conceptual model structure, parameter equifinality and the choice of calibration period (wet, dry). He used two different model structures and 100 equifinal parameter sets sampled by Monte Carlo sampling and two emission scenarios, and found that the uncertainty on projected monthly mean river flows due to parameter equifinality was higher in winter than summer and comparable to those related to emission scenarios. Kay et al. (2009) used two different versions of a conceptual model and a jackknifing method to generate parameter sets and found that the uncertainty related to climate modeling was higher than that arising from hydrological modeling. In a snow-dominated basin of southern Québec, Poulin et al. (2011) used two hydrological model versions and equifinal parameter sets obtained by multiple calibrations with the SCE-UA algorithm, and found that model structural uncertainties are more important than parameter uncertainty due to equifinality under climate change, insisting that this structural uncertainty should be considered in hydrological impact assessment studies. Bennett et al. (2012) used 25 Pareto solution sets obtained by the multi-objective algorithm MOCOM and found that hydrological parameter uncertainty was less than the uncertainties related to GCMs and emissions scenarios for three snow-dominated basins in British-Colombia, Canada. Ficklin et al. (2014) examined the effects of parameter equifinalty on hydrology in the SWAT model using outputs from five GCMs and showed that equifinal sets can lead to statistically significant differences in projected streamflow, snowmelt rates and timing under climate change. Hence the use of a single parameter set to project future streamflow under climate change with the SWAT model was deemed to be not robust in snow-dominated basins. Brigode et al. (2013) tested two models, GR4J and TOPMODEL, on 89 catchments in France to study the uncertainties related to parameter instability (dependence to calibration climate conditions) and parameter equifinality in a climate change context. They used the GLUE method to identify 2000 posterior parameters sets and found that the uncertainty arising from the temporal transferability of parameters was higher than that from equifinality. Her et al. (2016) studied the uncertainties related to climate models and hydrological parameter equifinality under climate change using the GLUE method and different thresholds to identify behavioral parameter sets. They showed that parameter uncertainty depends on the choice of hydrologic indicator and has a greater influence on soil moisture and groundwater projections than climate model uncertainty. Foulon et al. (2018) assessed the impact of equifinality and the choice of objective function on several hydrological indices, including SWE and maximum winter peak flows. Their study was conducted over 10 basins in Québec with the Hydrotel model, using 250 equifinal sets and different objective functions computed on streamflow. They found that the choice of objective function was most important for SWE, while parameter equifinality was a more important source of uncertainty for the other hydrologic indices. The authors insisted that equifinality should be systematically taken into account in future work. Most of the aformentionned studies compared the sources of uncertainty and demonstrated that uncertainties induced by hydrological models are less important than climate models, but nonetheless suggested that they should be evaluated when performing climate change impact assessments.

The main question of interest in this study is whether simple conceptual hydrological models are capable to adequately simulate runoff as well as snow cover in snow-dominated basins and how stable are the optimized parameters. Therefore, the main objective of this study is to improve the simulation of snowpack by a parsimonious hydrological model, GR4J (Perrin et al., 2003), coupled to the snow model Cemaneige (Valéry, 2010) by considering available SWE observations from the Quebec permanent snow measurement network in the model calibration. We further investigate different calibration strategies, by (i) comparing the respective performance of a local, global and multi-objective algorithm for twelve snow-dominated basins in Québec, and (ii) comparing how the calibration strategy improves the parameters identifiability. Finally, we test how the uncertainty related to parameter equifinality impacts the assessment of streamflow sensitivity to climate change. The goal is not to perform a thorough, scenario-based climate change impact assessment nor to compare the different sources of uncertainties, but rather to focus on the impacts of choosing either a mathematically-optimal parameter set versus several equifinal parameter sets on the detection of a climate changing signal in selected streamflow signatures.

Data and methods

Study site and data

Twelve tributary basins of the St. Lawrence River in Quebec were selected in this study (Fig. 1). The choice was based on the length of observed discharge data (> 20 years), the natural character of the hydrological regime of the rivers and, especially, the availability of snow measurement points inside or close to the studied basin. The area of the basins varies between 367 and 4504 km^2 (Table 1). They are located in four homogeneous hydrological regions, namely (i) the St. Lawrence northwest region (Batiscan, Bras du Nord, Matawin) on the north shore and characterized by a continental climate; (ii) the St. Lawrence southwest region (Nicolet, L'Acadie) characterized by a mixed maritime and continental climate; (iii) the St. Lawrence southeast region (York, Beaurivage, Bécancour, Famine, Etchemin, Ouelle) characterized by a mix of maritime and continental climate, and (iv) the St. Lawrence northeast (Godbout) characterized by a maritime climate (Assani et al., 2010a; Assani et al., 2010b; Mazouz et al., 2013).

Daily historical discharge data measured at the basin outlets were extracted from the website of the Quebec Center of Water Expertise (CEHQ) (www.cehq.qc.ca). The climatic data used were extracted from the daily climate grids developed by the Atmospheric Environment Information Service (SIMAT) in collaboration with the CEHQ (Bergeron, 2015). The total daily precipitation (solid and liquid), minimum and maximum temperature at each grid point are estimated by spatial interpolation (kriging) using stations managed by the Quebec Climate Monitoring Program (Programme de surveillance du climat du Québec: PSC) and stations operated by the national hydropower company Hydro-Québec. The interpolated climate grids are considered to be of good quality in the southern part of Quebec given the high density of stations in this region. Continuous data are available for the period from 1961 to 2015 (Bergeron, 2015). The snow observations come from the permanent snow survey network maintained by the Ministry of Environment and Fight Against Climate Change (MELCC). Survey sites are located in forested areas where the depth and density of snow is measured every two weeks during the winter and spring seasons. Each SWE observation at a given survey site represents the average of ten manual measurements made with a snow tube along a 100 m-long transect. The historical measurements of 12 survey sites located in or very close to the selected basins were used. The snow survey sites and the characteristics of the basins are shown in Table 1.

Models

The GR4J (modèle du Génie Rural à 4 paramètres Journalier) hydrological conceptual model (Perrin et al., 2003) and the Cemaneige snow model (Valéry, 2010) were chosen in this study to simulate the snow cover and hydrology of the basins. In the GR4J model, hydrological processes in the basin have been simplified into two interconnected reservoirs. The production function, which determines the amount of water in the basin, is represented by a soil reservoir with a maximum capacity x1 (mm) which is the first parameter to be calibrated. The transfer function, which determines the transfer of water in the water basin, is represented by a routing reservoir which receives the quantity released by the production function and calculates a discharge linked to its level of filling and its maximum retention capacity at 1-day, x3, which is a free parameter. Edijtano (1991) added a function to simulate water transit time to the routing reservoir by a unit hydrograph to improve the simulation of flood peaks in which 90% of the water released by the production store is routed by a unit hydrograph to the routing reservoir, while the remaining 10% contributes directly to flow and is routed only by a unit hydrograph. The base of the unit hydrograph, x4 (mm/day), is a free parameter. The model was previously found to give poor simulations in basins with intermittent flow regimes. For this reason, Nascimento (1995) added a groundwater exchange function to the routing reservoir and to the direct flow component which improved runoff simulations. This exchange coefficient, x2 (mm/day), can be negative (losses to the aquifer) or positive (inflow from the aquifers) and this is why the model no longer considers the basin as a conservative water balance system but rather as an open system (Perrin, 2000; Perrin et al., 2003; Perrin et al., 2007). The version of GR4J from Perrin (2000) is used in this study.

Developed by Valéry (2010), the Cemaneige module with two free parameters simulates snow accumulation an melt in the basin with one snow reservoir for each of five altitude bands. The two internal states of the snowpack simulated are the snow storage (snow water equivalent) and the thermal state. The snow storage is initially zero and increases at each time step after adding the solid fraction of the precipitation. The thermal state of the snowpack (°C) determines the onset of melting and is calculated by a weighting coefficient, x5 (dimensionless), which is a free parameter of the model to be calibrated and varies between 0 and 1. A value of 1 describes a maximum thermal inertia of the snow compared to air temperature. After the calculation of the snow storage and its thermal state, the model calculates the potential melt which represents the maximum amount of snow that can melt using the degree-day method. The degree-day factor, x6 (mm $°C^{-1}$), controls the potential melt and is a free parameter to be calibrated. Six parameters must then be calibrated for the coupled GR4J-Cemaneige model. Table 2 summarizes the description of these parameters. The ranges of hydrological model parameters are based on literature and previous studies (Perrin, 2000) while those for the Cemaneige model were chosen based on the work of Valéry (2010).

Calibration strategies

In the calibration strategy, the choice of optimization algorithm and objective functions have a great influence on the identification of the parameters and their uncertainty, in addition to the structure of the model and the quality of the input data. The objective of improving the snow cover simulation by the GR4J-Cemaneige model and the identifiability of the parameters led us to consider four calibration strategies in which three algorithms (local, global and multi-objective) were used: for the first two strategies, the calibration of the six GR4J-Cemaneige model parameters was done simultaneously using the observed discharge, with respectively a local 'pas-à-pas' approach (strategy 1: 'LOCAL') and the global SCE-UA algorithm (strategy 2: 'SCE-FLOW'). The local 'pas-à-pas' (step-by-step) optimization algorithm was used for the development and improvement of the two models by researchers at Cemagref, France (Perrin, 2000). The global automatic algorithm Shuffled Complex Evolution (SCE-UA) developed by Duan et al. (1992) is considered the most efficient by hydrologists. The SWE simulated by these two strategies was then compared with the SWE observed at the nivometric survey points in, or closest to, the selected basins, for the elevation band closest to the elevation of the snow survey point. In the third strategy, 'SCE_INDEP', the four hydrological model parameters and the two snow parameters were calibrated separately. The two snow parameters were calibrated with the observed SWE and prescribed subsequently as fixed parameters in the coupled GR4J-Cemaneige model. The four hydrological parameters were next calibrated with the observed discharge by the global SCE-UA algorithm. The fourth and final multi-objective strategy, 'MULTI', was finally applied in which the six model parameters were calibrated simultaneously with the observed SWE and discharge using the multi-objective optimization algorithm AMALGAM (Vrugt et al., 2007). The split-sample test calibration method (Klemes, 1986) was used to separate the observation record into two equal length periods of calibration/validation (Table 1). The Nash-Sutcliffe (1970) efficiency criterion was used as the evaluation criterion and calculated from the observed and simulated discharge (Nash-Q) and from the SWE measured at surveys point and that simulated by the model for the corresponding elevation band (Nash-SWE):

$$Nash\text{-}Q\ (Q) = 100\left[1 - \frac{\sum_{i=1}^{n}(Qo_i - Qs_i)^2}{\sum_{i=1}^{n}(Qo_i - \overline{Qs_i})^2}\right] \qquad \text{Equation (1)}$$

$$Nash\text{-}SWE\ (SWE) = 100\left[1 - \frac{\sum_{i=1}^{n}(SWEo_i - SWEs_i)^2}{\sum_{i=1}^{n}(SWEo_i - \overline{SWEs_i})^2}\right] \qquad \text{Equation (2)}$$

where Qo and Qs are the observed and simulated discharge and SWEo and SWEs the observed and simulated snow water equivalent, respectively.

Parameters equifinality

Only the calibration methods SCE_FLOW and MULTI were used in this step to study the interaction and the compensation between parameters. Iterations made by the algorithms during calibration until convergence were saved (more than 6000 for each basin). For the SCE-UA algorithm, the parameter sets yielding a Nash value within 1% of the optimal Nash value were considered equifinal. Similarly, for the multi-objective algorithm AMALGAM, the optimal point of the Pareto solution was chosen and all parameter sets around this point that gave the same optimal performance with a difference less than 1% in the Nash criterion were retained.

Parameter sensitivity analysis

The dynamic identifiability analysis (DYNIA) method developed by (Wagener et al., 2003) was used after that to investigate the parameter identifiability. This method consists in testing the identifiability of each parameter in a moving time window, set to 15 days here, by identifying the portion of the parameter range that give the best performance (Wagener et al., 2003). Finding a clear range of parameter values that give the best simulation means that this parameter is more identifiable in this time window, while the opposite means that all values within the range can give equally-best simulation in combination with other parameters. Time-varying sensitivity analysis (TVSA) (Pianosi et al., 2016; Reusser et al., 2011) is used also to investigate the most influential model parameters at each time step of the simulation and the consistency of the parameter role and its period of influence with the physical behavior of the basin (Pianosi et al., 2016; Reusser et al., 2011).

Climate sensitivity

The objective in this step is to assess how parameter equifinality and the choice of a single optimal parameter set versus several equifinal sets impact the characterisation of streamflow sensitivity to climate change. We focus here on the sensitivity of the average annual springtime peak streamflow ($Qmax_{sp}$) and its timing ($Qmax_{sp}T$) to a +2 °C increase in mean air temperature. Only the equifinal sets obtained by the third calibration strategy, the most used in literature, was considered in this part (SCE-FLOW). The sensitivity measures used (ΔQmaxsp), is the percent difference between the mean historical $Qmax_{sp}$ obtained by the optimal set and that projected by the optimal set and equifinal sets under the warming scenario. The same approach was used for the peakflow timing (ΔQmaxspT, in days). The objective is to investigate the agreement between the equifinal and optimal sets about the evolution, i.e. the direction and magnitude of change, of an important hydrological indicator in southern Quebec which is the peak streamflow induced by snowmelt in spring.

Results

Models performance

For all calibration strategies, one global optimal parameter set was obtained, except for the multi-objective method MULTI where a vector of 'Pareto-optimal' parameter sets was obtained. The optimal point of the Pareto set that gives the best compromise between snow SWE and discharge was selected to compare with the performance of the other calibration strategies. Boxplots in Fig. 2 show the model performance for the 12 selected basins and the four calibration methods for both the calibration and validation periods. With the first method LOCAL (Fig. 2a1) the model shows a good performance in discharge simulation with a median Nash-Q value of 84%

in calibration and 80% in validation but a comparatively poor performance in SWE simulation: the median Nash-SWE value is around 40% during calibration and increases to 58% in validation, but the spread of the distribution is higher (Fig. 2a2). The calibration results with the global algorithm SCE_FLOW also show a good streamflow simulation with a median Nash-Q value of 82% in calibration, similar to the first method, but with an improvement in validation with the median Nash-Q value increasing to 83% (Fig. 2b1). The SWE simulation is still weak with the SCE_FLOW method but slightly improves nonetheless with the median Nash-SWE value increasing to 43% in calibration and 59% in validation (Fig. 2b2), but the spread of the distributions is still considerable and comparable to the first local method. In the third strategy SCE_INDEP, the two Cemaneige parameters were calibrated separately against the observed SWE, which improved significantly the Nash-SWE in calibration with a median value of 58%. This significant improvement in the Nash-SWE criterion is however accompanied by a degradation of the flow simulation, with the median Nash-Q value decreasing to 80% in calibration and 76% in validation, which means that the introduction of two fixed snow parameters in the GR4J-Cemaneige model led to an over-adjustment on the SWE and a degradation in the streamflow simulation (Fig. 2c). The multi-objective strategy in which the Nash-SWE and Nash-Q are simultaneously optimized (Fig. 2d) improved the simulation of the SWE, with 75% of the basins having a Nash-SWE greater than 50% in calibration and greater than 40% in validation, without significantly degrading streamflow simulations (Fig. 2d1). The simulation of SWE is hence significantly improved for the two methods SCE_INDEP and MULTI in which the snow observations are taken into account (Fig. 2c-d), but the method SCE_INDEP degrades the simulation of discharge. The best simulation of SWE in both calibration and validation without significant streamflow degradation is obtained by the MULTI method, for which the model efficiency ranged between 31 and 84% for the 12 basins (Fig. 3). The best SWE simulations were obtained for the Famine, Beaurivage, Ouelle, Bécancour, and Bras de Nord basins, with a Nash-SWE criterion above 65% while the poorest simulation were obtained for the Matawin and Acadie basins. The poor simulation in these two basins may be due to the survey sites being less representative of the basin, which is an obvious limitation of using point observations to constrain the snow model. Fig. 4 shows an example of SWE simulation for the Bécancour catchment with the MULTI method.

Parameters interaction

The distribution of the optimal parameters obtained for the 12 basins is different between the calibration strategies, except for the parameter x4 (base of the unit hydrograph) and x2 (water table exchange) which are more similar (Fig. 5). The choice of the calibration method does not seem to have a clear impact on the distribution of the parameters between the basins. For the third method SCE_INDEP, where the calibration of the Cemaneige parameters is done separately on the SWE observations, the degree-day factor x6 which determines potential snowmelt is higher and more dispersed than for the other methods, while x5 (weighting coefficient of the thermal state), which determines the onset of melting, is minimized. Subsequently, the parameter x1 (maximum capacity of the soil reservoir) approaches its lower limit in some basins while x3 (the routing reservoir capacity) approaches its upper limit. The optimal parameters obtained by each calibration strategy differ with each other for a given basin (Fig. 6). This shows that different optimal sets give the best simulation for each calibration method over the same period. The two parameters x2 and x4 are the only ones for which similar values are obtained from all calibration strategies.

Equifinality was studied using two calibration methods, namely SCE_FLOW, which is the global algorithm most used in the literature and uses only observed discharge, and the method MULTI which gave the best performance (Fig. 3). The distributions of equifinal parameters obtained for the 12 basins by the procedure described in the methods section are presented in Fig. 7. The distributions for the SCE_FLOW method are narrow but with many extreme values, while the distributions for the multi-objective method are more homogeneous (Fig. 7). For the SCE_FLOW method the number of sets found is very high and variable between basins. Therefore, in order to converge mathematically with a very small change in the Nash value (< 1%), the maximum capacity of the soil reservoir (x1) can, for example, vary from 200 to

450 mm for basin 1 (Batiscan). Similar variability is seen for the other basins. The calibration with the multi-objective algorithm reduced the number of equifinal parameters sets and their dispersion (Fig. 7b). The MULTI method also reduced the range, i.e. the difference between the maximum and minimum parameter value, but no significant reduction was found in the interquartile range compared to the SCE_FLOW method (Fig. 8). The correlation between the equifinal sets can explain this dispersion and multiplicity of parameters giving the same performance. A strong negative correlation is found between the two reservoir parameters, x1 (the maximum soil reservoir capacity) and x3 (the routing reservoir capacity), with a median value of -0.7, and between the two transfer parameters x3 and x4 (base time unit hydrograph) with a median value of -0.5 (Fig. 9). A positive correlation is also visible between x1 and x2, which regulates the amount of water available in the basin, with a median value of 0.4 (Fig. 9a). This strong correlation shows the compensation between the parameters occurring during the optimization and the difficulty to converge toward an optimal set. This parameter correlation was significantly reduced when using the MULTI method (Fig. 9b).

Identifiability analysis of GR4J-Cemaneige parameters

The equifinality of parameters has led us to investigate more deeply the identifiability of the GR4J and Cemaneige parameters using the DYNIA and TVSA methods in order to understand the interaction of model parameters. The analysis was only performed in the Bécancour basin (ID#2) for the sake of brevity. The temporal identifiability of the six parameters of the GR4J-Cemaneige model found by the DYNIA method is shown in Fig. 10. In these graphs the color scale represents the frequency distribution of the parameters for a sample of the 10% best-performing simulations, using the root-mean-squared error (rmse) as objective function. A parameter becomes more identifiable during periods when the frequency distribution is narrower. For the parameter x1, low values are more frequent before and during floods, while high values are more frequent after the floods. There is no clear part in this parameter space that is identifiable in the best-performing simulations, which indicates that different values of this parameter give similar results in combination with the other parameters. Parameter x2 is a multiplicative parameter that regulates the volume of water in the basin: the more positive its value, the largest is the contribution of groundwater to the basin, while more negative values increase deep percolation losses. Fig. 10 shows that negative values are more frequent during low flow periods, indicating large water losses to deep aquifers simulated by the model. Conversely, high positive values of x2 are more frequent during floods. This means that to simulate the high flows the model increases the supply from the water table while for the low flows the model increases the loss to the water table. The high sensitivity of x2 implies that the GR4J model first tries to use this parameter to adjust the water volume in the basin and then the other production parameter x1, which explains the difficulty of finding sensitive x1 values conditioned on discharge. The parameter x3 (one-day capacity of the routing reservoir) is barely identifiable: high values are more frequent during and before the floods, and after the floods the models begins decreasing the its value but still the identifiability is unclear. The identifiability of the parameters x4 (base time of the unit hydrograph) and x5 (thermal coefficient of state of the snowpack) is low since very different values of these parameters give similar results in combination with the remaining parameters. Parameter x6 (degree-day factor) is somewhat identifiable during the melt period, with a value between 5 and 7 mm $°C^{-1}$ giving the best simulation. Time-varying sensitivity analysis (TVSA) (Reusser et al., 2011) (Fig. 11) also shows that the parameter x2 is the most influential, except during the spring pre-flood periods when the snow parameters x5 and x6 of the Cemaneige model become the most influential, whereas they have no influence on the rest of the period. This confirms that the behavior of the model is consistent with the physical behavior of the basin in the spring. The sensitivity of x1, x3, and x4 is not clear compared with x2, suggesting that the model tries to first use the x2 parameter value to adjust the flow and then uses the other parameters afterward.

Equifinality under changing climate

The final objective of this study was to assess how parameter equifinality and the choice of a single optimal vs. equifinal parameter set impact the characterisation of streamflow sensitivity to climate change. The distribution of $\Delta Qmax_{sp}$ values can thus be used to quantify the uncertainty in the sensitivity of springtime peak flow to warming which results from equifinality alone (Fig. 12) There is a general agreement between all equifinal and the optimal sets that peak spring streamflow would decrease in the future in response to a +2 °C climate warming, as all simulations display negative $\Delta Qmax_{sp}$ values. For all basins the impact of a +2 °C climate warming on $Qmax_{sp}$ can be detected using the optimal parameter set (red dot on Fig. 12) with a 99% confidence interval varying between ± 0.8% (basin 10) to ± 3.9% (basin 7), which is a rather low uncertainty. However, the distributions of sensitivities is not normal, and when we take into account all the parameter sets including the numerous outliers, the range of reduction in $Qmax_{sp}$ can be much greater, as much as 12% (-10 % to -22%) for basin 3 and 13% (-4% to -17%) for basin 11. The difference of uncertainty between basins can be explained by the dispersion of equifinal parameters displayed in Fig. 7: basins with the most dispersed equifinal parameter distributions (ID# 1, 3, 11) have the largest errors in their temperature sensitivities.

There is an agreement, except for basin 12, that peak springtime streamflow will occur earlier in response to a +2 °C temperature warming (Fig. 13). For basin #2 the peak streamflow could occur earlier by 2 to 10 days and for the two basins #7 and #8 the occurrence day could shift earlier by 3 to 9 days depending on the equifinal parameter set. For basin #12 (L'Acadie River), which is the southernmost basin studied (Fig. 1), the change in peakflow timing detected using the optimal parameter set is positive but the uncertainty due to equifinality, when considering outliers, is such that the direction of change in timing cannot be reliably detected for this basin.

Discussion and conclusion

SWE simulation

Having a good simulation of streamflow generated by snowmelt has always been an important objective of hydrologists during the development of snow models to be used within hydrological models, and their performance has been generally assessed by their capacity to simulate observed streamflow, which was the case for the development of the Cemaneige model (Valéry, 2010). The objective is most often to obtain the best efficiency criteria between observed and simulated streamflow, which does not always guarantee that other processes such as snowmelt are properly simulated by conceptual models. The contribution of this study was mainly to test the use of snow survey points to improve the calibration of the conceptual models GR4J and Cemaneige while avoiding the difficulties related to snow cover satellites products. Four calibration strategies have been tested for the simulation of discharge and SWE using a local, global and multi-objective algorithm. After comparing results obtained by the different methods, it appears that overall the calibration against observed discharge in the first two methods yielded good streamflow simulations but poor simulations of SWE. The global algorithm SCE-UA yielded a better streamflow simulation in validation that the local algorithm, confirming previously reported results about the ability of global algorithms and specifically the SCE-UA to find global optimal parameters, unlike the local algorithms that depend on initial sets (Efstratiadis et al., 2010). Despite this mathematical power of the SCE-UA algorithm in finding the global optima, its performance in simulating SWE was very similar to the local algorithm. On the other hand, the separate calibration of the snowmelt model in the third method showed an over-adjustment of the model to the SWE simulation and a subsequent significant degradation of the streamflow simulation compared to the first two methods. The multi-objective calibration against both observed runoff and SWE using the AMALGAM algorithm gave the best simulation of SWE, with a very small degradation of runoff simulation compared to the streamflow-only calibrations approaches. Troin et al. (2015) also used the same third strategy SCE-FLOW (calibration against discharge with SCE-UA algorithm) over one catchment in Quebec (Mistassibi Basin) to test different combinations of seven snow models and three hydrological models including GR4J-Cemaneige, and used four SWE measurement points to compare with the simulated SWE. They found a good simulation of streamflow as well as good performance for SWE simulations with all model combinations including GR4J-Cemaneige (Nash = 79%). This disagreement with our results can be explained by the results displayed in Fig. 5: good SWE simulations are found with this strategy for some basins, but overall for the twelve basins studied and comparing with the multi-objective approach this method does not give a good simulation of SWE. Therefore, we emphasize that the general model performance should be evaluated on several basins.

Overall, the results of this study show that the additional information provided by the snow survey points improved the simulation of SWE without degrading the streamflow simulated by the conceptual rainfall-runoff GR4J coupled with the snow model Cemaneige. This type of snow data has only been exploited in a few studies for the calibration of hydrological models (Troin et al., 2015; Turcotte, 2010; Turcotte et al., 2010; Turcotte et al., 2003). On the other hand many previous studies have already shown the effectiveness of using remotely-sensed snow cover data in several regions of the world for the calibration of hydrological models using a multi-objective approach (Duethmann et al., 2014; Finger et al., 2011; Gupta et al., 2003a; Hogue et al., 2003; Madsen, 2003; Parajka et al., 2008; Parajka et al., 2007; Roy et al., 2010; Turcotte ebt al., 2003). Given that the satellite-derived SWE by microwave methods is still difficult in Quebec with deep snowpacks and dense forests (Bergeron et al., 2014; Brown, 2010; Sena et al., 2016), our results show that including snow survey observations could be a good alternative for the calibration of conceptual models in snow dominated basins. These observations could even be used conjointly with remotely sensed data to improve the simulation in forested basins. Moreover, our results show that using complementary snow data improves the physical realisms of conceptual hydrological models and strengthens the confidence in using these models to project climate change impacts on hydrology.

Equifinalty and model structure uncertainty

We considered as equifinal parameters in this study the iterations during the optimization by the algorithms SCE-UA and AMALGAM that gave the same optimal Nash criteria, within a small 1% difference. The large number of equifinal sets and their dispersion for a < 1% change in the objective function (Nash criterion) reveals the difficulty of the algorithm to converge toward one clear optimum. For the SCE-UA algorithm, the maximum soil reservoir capacity x1 was found to be negatively or positively correlated with the exchange coefficient x2 and the maximum capacity of the routing reservoir x3 (Fig. 9). Therefore these three parameters can play the same role to adjust the water balance in the basin as a quantity of water can be stored in the soil reservoir, routing reservoir or infiltrated into the water table by the parameter x2. Lay (2006) used sensitivity analysis and found that the model is respectively more sensitive to the soil reservoir capacity x1, the parameter of the unit hydrograph x4, the ground water exchange parameter x2, and the routing reservoir capacity x3. A correlation has already been found by Perrin (2000) between the parameter sets obtained by multi-calibration on many subsets, namely a significant correlation between x2 and x1 and also between x3 and x1. He explained this multiplicity of parameters by the dependence between the parameters and the climatic conditions of the calibration period, as already proposed by several other authors (Coron et al., 2014; Merz et al., 2011; Seiller et al., 2012; Vos et al., 2010). The low identifiability of model parameters appears when the change in the value of a parameter is compensated by changes in other parameters. The analysis by the DYNIA method (Fig. 10) confirms these results and shows that for all parameters the model always struggles to find a range of parameter values which is identifiable, except for the exchange coefficient (x2) which is the loss or gain of water to the water table. This confirms the results of Perrin (2000), that the model GR4J could use the exchange parameter x2 more than the soil reservoir x1 to adjust the basin water balance.

Several studies have discussed the importance of multi-objective strategies in which another hydrological process is added to calibration in order to constrain feasible parameters, reduce equifinality and improving the identifiability of parameters (Gupta et al., 1998; Tang et al., 2006; Wagener et al., 2005; Wagener et al., 2003). Her et al. (2018) also used the AMALGAM algorithm and objective functions calculated on several streamflow criteria (without adding additional information) and demonstrated that equifinality and uncertainty decrease when the number of objective functions considered increases. This is consistent with our results which showed that adding observed SWE survey points to the AMALGAM algorithm reduced the number, dispersion and correlation of equifinal sets. Moreover, we found no correlation between the optimal parameter sets and the physical characteristics of the twelve basins studied, similar to the numerous previous studies that also failed in the regionalization of these parameters. Andréassian et al. (2012) discussed the difference between miscalibration, which is a numerical problem to be solved by sophisticated algorithms, and over-calibration, which is the difference between a mathematical and hydrological optimum related to the structure of the model. The low identifiability and strong interaction between the GR4J equifinal parameters demonstrated here, reveal the large compensation between the parameters which can be at the origin of equifinality, rather than the objective function or input data. Thereafter the conceptualization of hydrological processes using mathematical equations and the interaction of parameters should be the main reason for parameter non-uniqueness. As explained by Wagener et al. (2005), after many years of looking for the best model with a unique optimal parameter set, the emergence of the equifinality concept was the turning point toward a new paradigm in which model consistency is sought by taking into account uncertainties and accepting parameter equifinality, which yield many models that give a good representation of the basin. On the other hand, does the existence of a large range of soil reservoir capacity or routing schemes that give a good simulation undermines the physical representativity of these parameters? The question here is to what limits can we accept the equifinality of parameters that represent physical characteristics of the basin? Shin et al. (2015), using several screening methods to check the identifiability of conceptual rainfall-runoff models (GR4J, SIMHYD, Sacramento and IHACRES), demonstrated also that the main reason for parameters no-identifiability is not the input data nor the objective function, but rather the model structure. They recommended fixing the parameters for which the model is more sensitive, or adding new information such as snow or groundwater, within a multi-objective approach to reduce the non-uniqueness of parameters and improve their identifiability. They found similar results about the significant parameter interaction in the GR4J model.

The use of hydrological models under conditions different from those of the calibration period, as in climate change impact assessment or for seasonal flood forecasting, has always been confronted by problems of parameter uncertainty, non-stability and multiplicity. Using a conceptual hydrological model forced by GCM outputs to assess climate change impacts on hydrology, without taking into account hydrological and climatic uncertainties is indefensible as shown by different studies. Many studies have tried to compare and rank the importance of the various sources of uncertainty by comparing the spread in futures projections, but the quantification of uncertainties, their hydrological significance and how they affect decision-making in a climate change context remains an active field of study. Unlike other studies, the objective here was to evaluate the uncertainty that can result from using a single, best numerical optimal solution rather than a set of parameters that give the same performance, on the temperature sensitivity of spring peak flow in snow-dominated basins. In several previous studies parameters uncertainty ranked last in order of importance in a climate change context (Bennett et al., 2012; Kay et al., 2009; Seiller et al., 2014; Teng et al., 2011; Wilby, 2005; Wilby et al., 2006). In this study, uncertainties due to equifinality of ± 0.9 to ± 3.9% (99% confidence interval) were found between the basins, which is not negligible and can affect climate change impacts assessment. Further studies are needed in snow-dominated basins to see how much the uncertainties induced by the calibration of snow models with observed discharge affect the detection of climate change impacts on the magnitude and timing of spring peak flow.

Conclusion

The main objective of this study was to evaluate the capacity of the coupled GR4J and Cemaneige models to simulate snow water equivalent and streamflow over twelve snow-dominated basins in Quebec, Canada. Results showed that adding SWE observations within a multi-objective approach gave a good performance in the simulation of both SWE and streamflow. Equifinality was studied by retaining parameter sets resulting in a model performance within 1% of the mathematical optimum for the same calibration period. The resulting multiplicity of parameters thus only represents the difficulty faced by the algorithms to converge toward a mathematical best optimum due to parameters interaction and does not reflect their dependence to climatic conditions, as studied several previous studies (Coron et al., 2012; Merz et al., 2011; Vos et al., 2010). The importance of the coupled GR4J-Cemaneige structure no-identifiability as the source of the large number of equifinal parameters found in this study comes in the same line of conclusions advanced by several authors (Gupta et al., 2014; Kavetski et al., 2011; Shin et al., 2015; Wagener et al., 2005). In addition to the simultaneous improvement of SWE and streamflow simulations, the multi-objective approach narrowed the dispersion and the number of equifinal parameters and improved their identifiability. Our study showed that equifinality caused uncertainties in the sensitivity of streamflow to climate warming, which should be considered in climate impact assessment studies with conceptual models. Based on our results, the use of conceptual models calibrated on observed discharge only and forced with climatic scenarios for the assessment of climate change impacts on snow cover and spring flow is not recommended.

List of tables

Table 1. Characteristics of the 12 selected study basins.

ID	Catchment	Lat. (°)	Lon. (°)	Area (km^2)	Med. Elev. (m)	Discharge data	Snow survey site	Snow site elev. (m)
1	Batiscan	46.59	-72.40	4504	385	1967-2017	Lac-Édouard-2	381
2	Bécancour	46.31	-71.45	2163	273	1999-2017	Lyster	131
3	Godbout	49.33	-67.65	1577	368	1974-2017	Lac-Sainte-Anne	290
4	Nicolet	46.06	-72.31	1550	203	1966-2017	Chester	274
5	Matawin	46.68	-73.92	1387	481	1931-2017	Barrière-St Guillaume	390
6	Etchemin	46.69	-71.07	1152	382	1980-2017	Saint-Léon	330
7	Ouelle	47.38	-69.95	796	348	1982-2017	Sainte-Perpétue	450
8	Beaurivage	46.66	-71.29	708	152	1925-2017	Saint-Étienne	99
9	Famine	46.1	-70.3	696	377	1964-2017	Sainte-Rose	404
10	York	48.81	-64.92	647	482	1980-2017	Murdochville	131
11	Bras du Nord	47	-71.8	646	597	1965-2017	Rivière-Verte-Ouest	236
12	L'Acadie	45.39	-73.37	367	31	1979-2017	Hemmingford	68

Table 2. GR4J-Cemaneige free parameters and lower and upper bounds used in model calibration.

Parameters	Physical description	Unit	Min-max
x1	Maximum capacity of production reservoir	mm	20-1500
x2	exchange coefficient	mm/day	-5-10
x3	Maximum retention capacity of 1 day	mm	1-400
x4	Base of the unit hydrograph	day	0.8-4
x5	Coefficient of thermal state	-	0-1
x6	Degree-day factor	mm $°C^{-1}$	0-20

Table 3. The four calibration strategies adopted in this study.

Calibration strategies	Optimisation algorithm	Objective function
LOCAL	Locale 'pas à pas'	Nash-Q
SCE_FLOW	SCE-UA	Nash-Q
SCE_INDEP	SCE-UA	Nash-SWE; Nash-Q
MULTI	AMALGAM	Nash-SWE; Nash-Q

List of figures

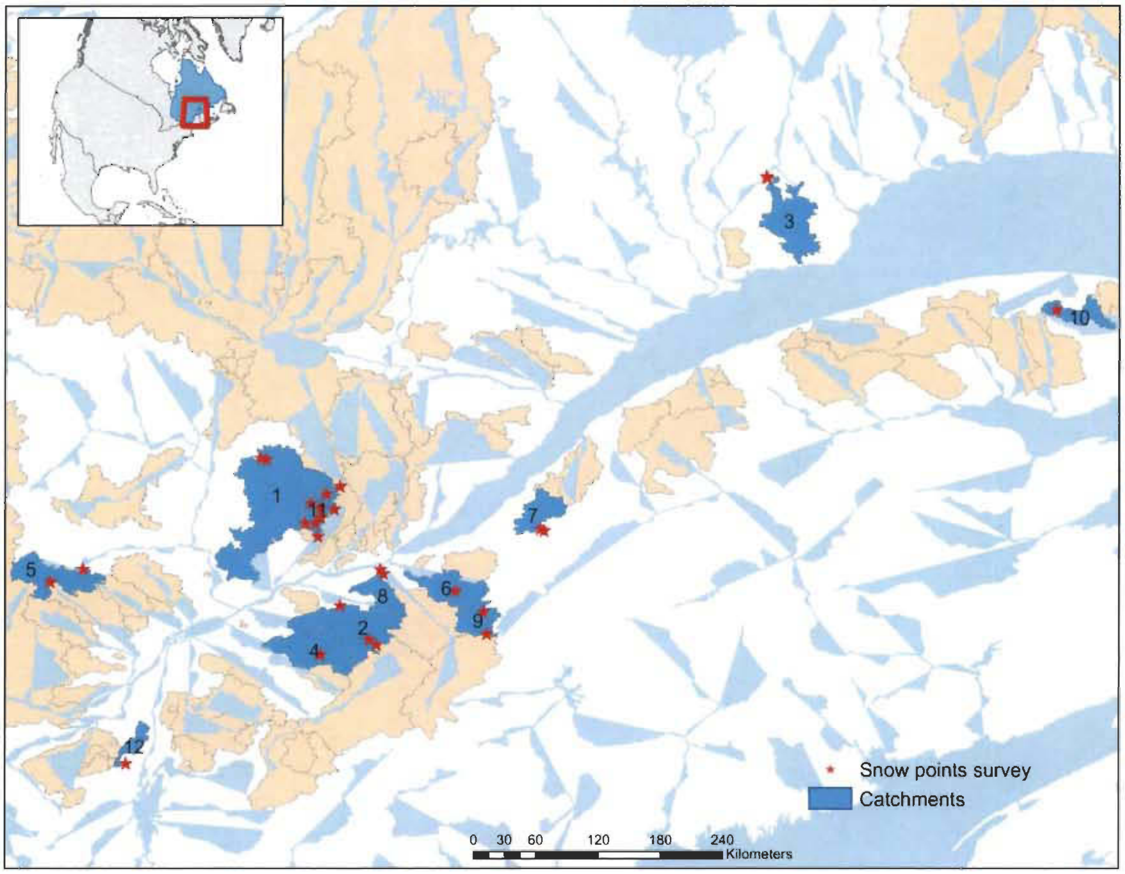

Fig. 1. Selected basins (blue) and snow survey measurement locations (red stars) in southern Quebec province. Basins ID ranked from largest to smallest basin area: 1 Batiscan, 2 Bécancour, 3 Godbout, 4 Nicolet, 5 Matawin, 6 Etchemin, 7 Ouelle, 8 Beaurivage, 9 Famine, 10 York, 11 Bras du Nord, 12 Acadie.

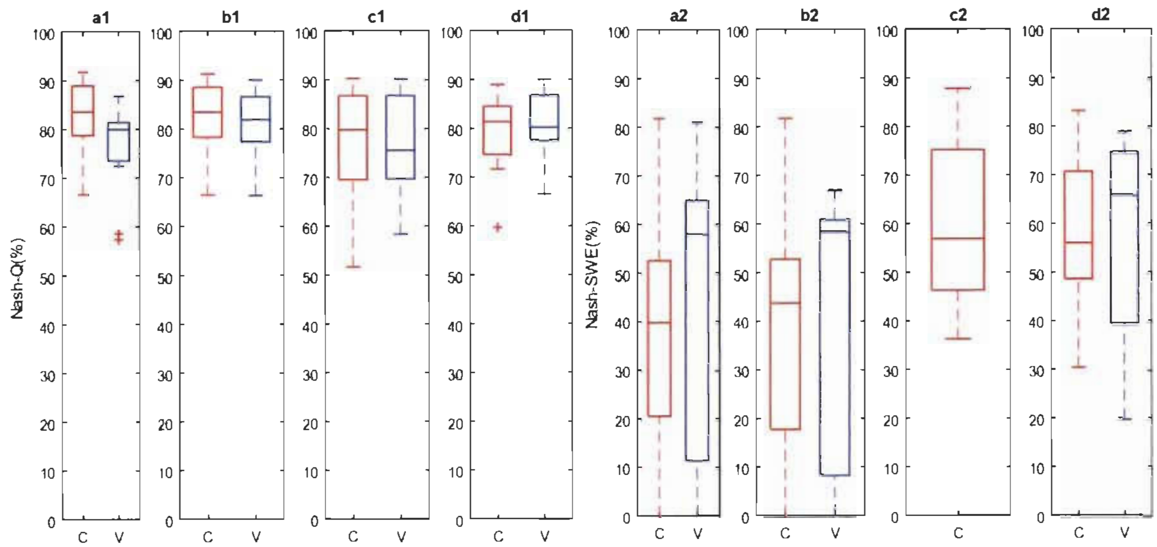

Fig. 2. Performance of GR4J-Cemaneige for streamflow simulation (a1-d1) and SWE simulation (a2-d2) for the calibration period (red boxplots) and validation (blue boxplots) for the 12 catchments using four calibration strategies: a: LOCAL; b: SCE_FLOW; c: SCE_INDEP; d: MULTI, C: Calibration, V: Validation.

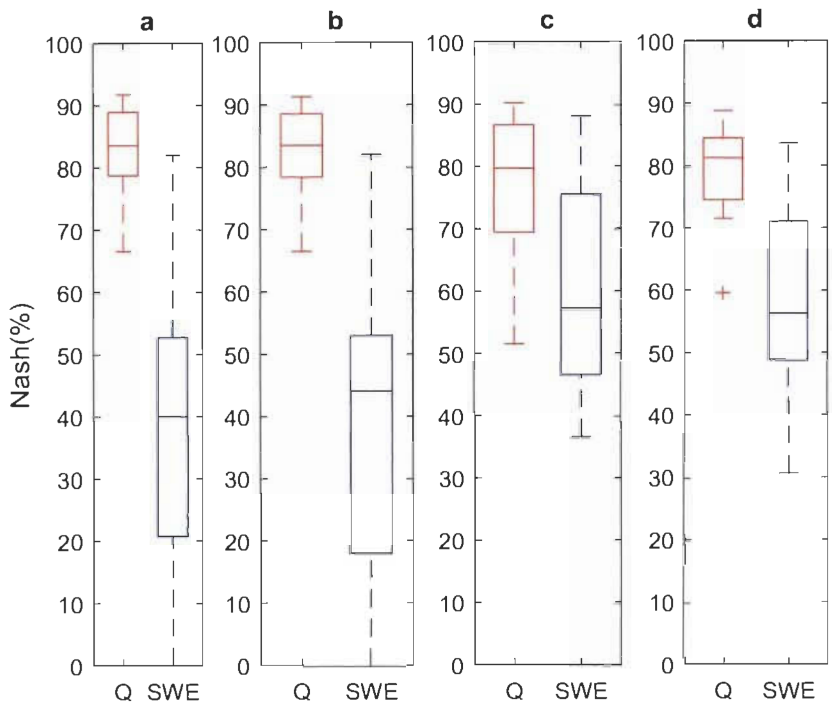

Fig. 3. Comparison of the calibration performance using calibration strategies: a: LOCAL, b: SCE_FLOW, c: SCE_INDEP, d: MULTI. Q: discharge (red boxplots); SWE: snow water equivalent (blue boxplots).

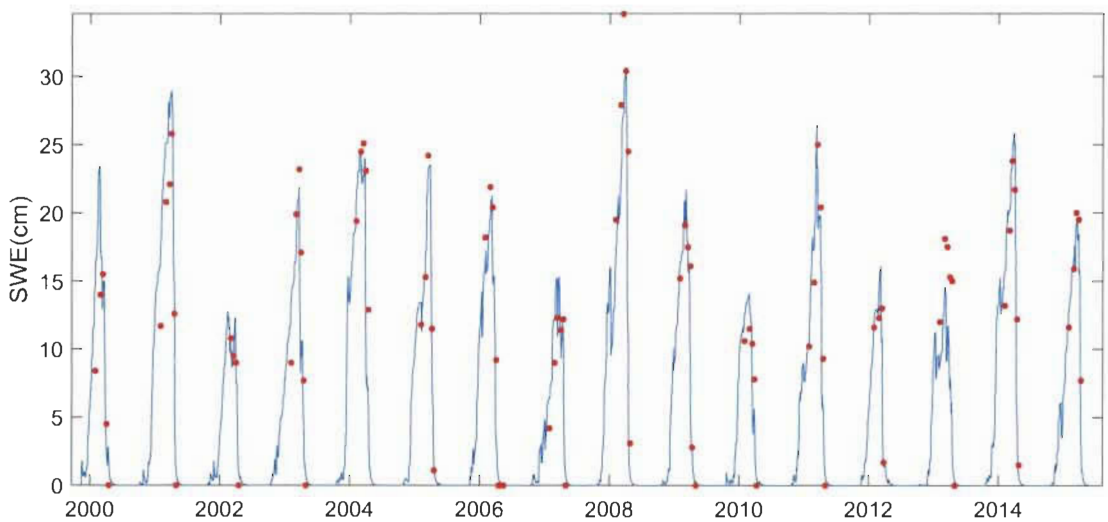

Fig. 4. Calibration results for snow water equivalent (SWE) by the multi-objective 'MULTI' method for the Bécancour catchment (ID#2); Red dots: measured SWE; blue line: SWE simulated by the Cemaneige model.

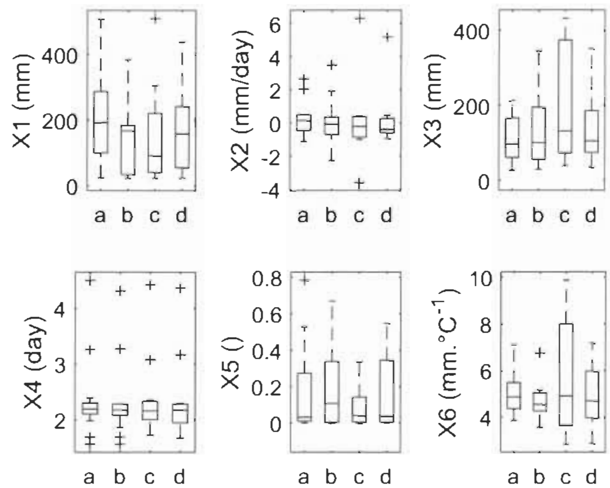

Fig. 5. Distribution of optimal parameters sets obtained for the 12 basins by the four calibration strategies: a: LOCAL, b: SCE_FLOW, c: SCE_INDEP, d: MULTI.

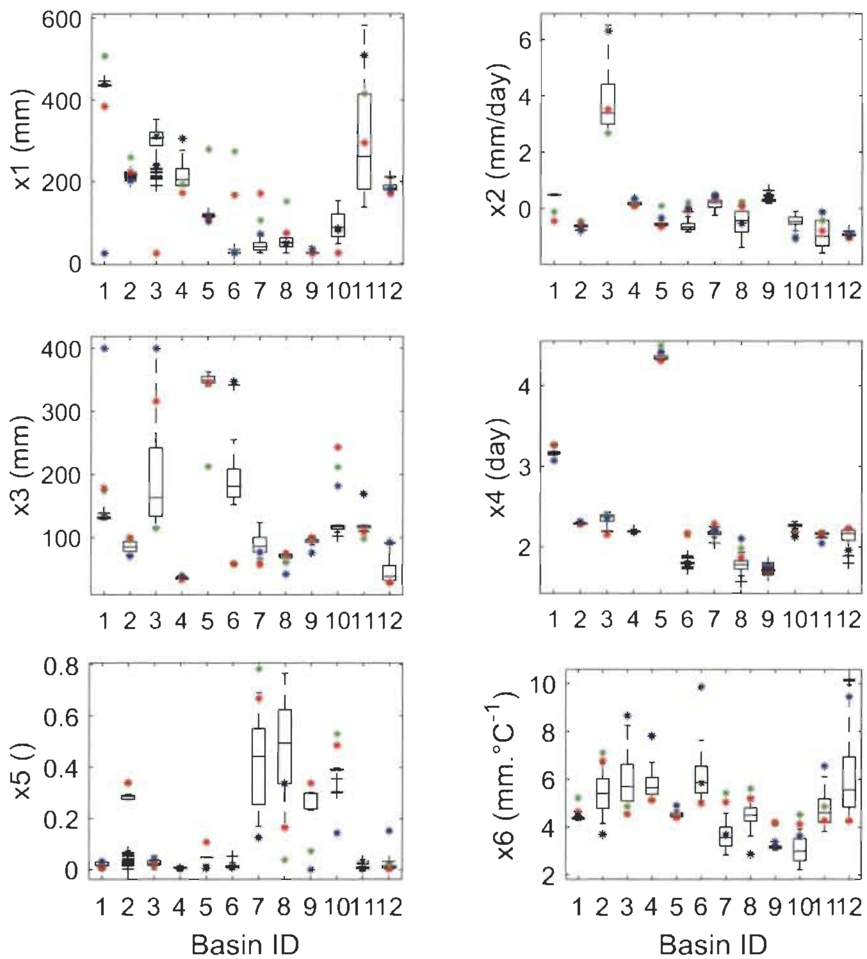

Fig. 6. Boxplots of Pareto solutions vector (100 sets) obtained by the multi-objective calibration method 'MULTI' for each basin. The coloured dots represent the optimum parameter sets obtained from the other calibration methods. Red dots: SCE_Flow; blue dots: SCE_INDEP; green dots: LOCAL.

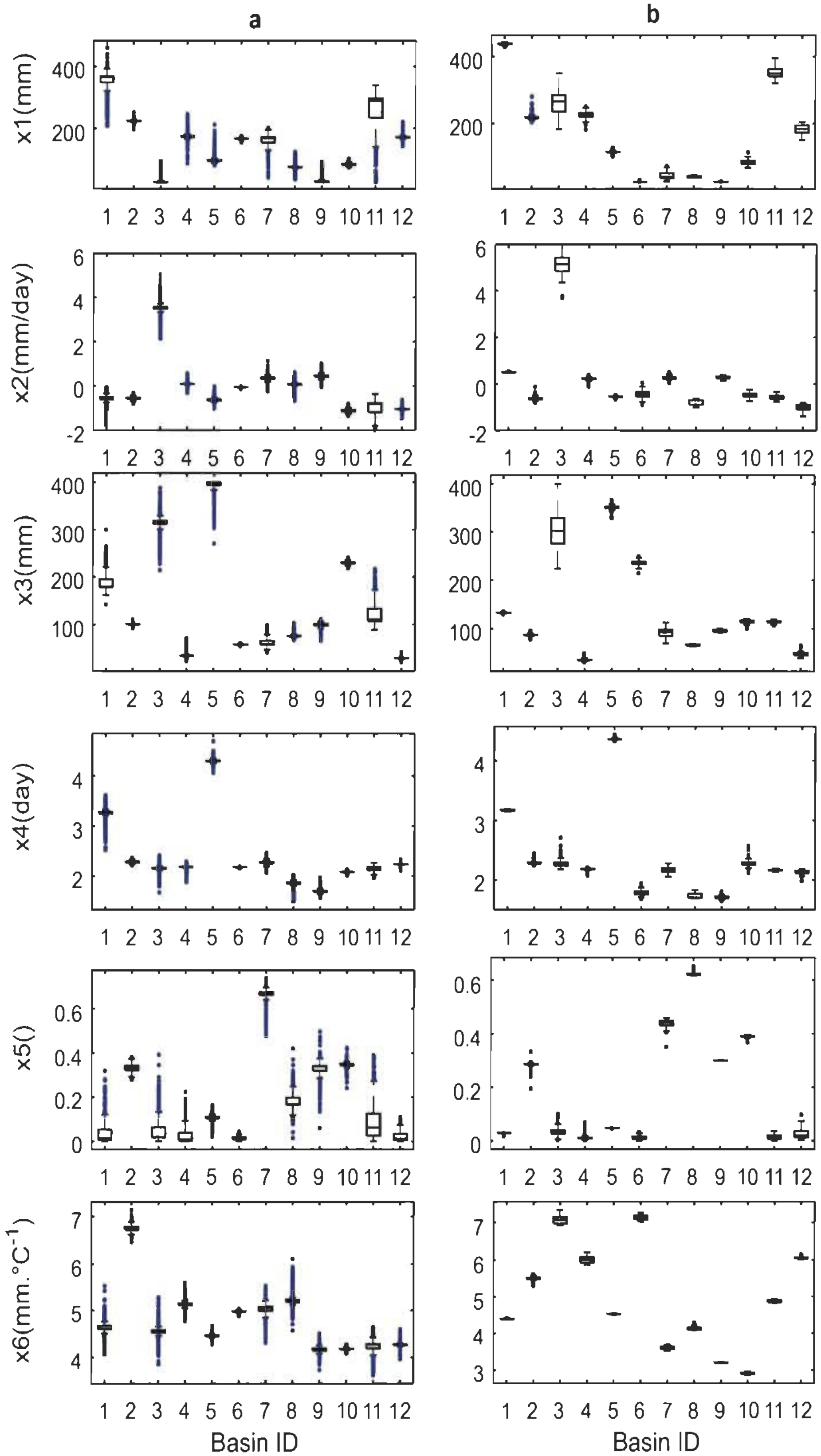

Fig. 7. Boxplots of equifinal parameters sets for the twelve basins using the two calibration methods: A: SCE_FLOW B: MULTI.

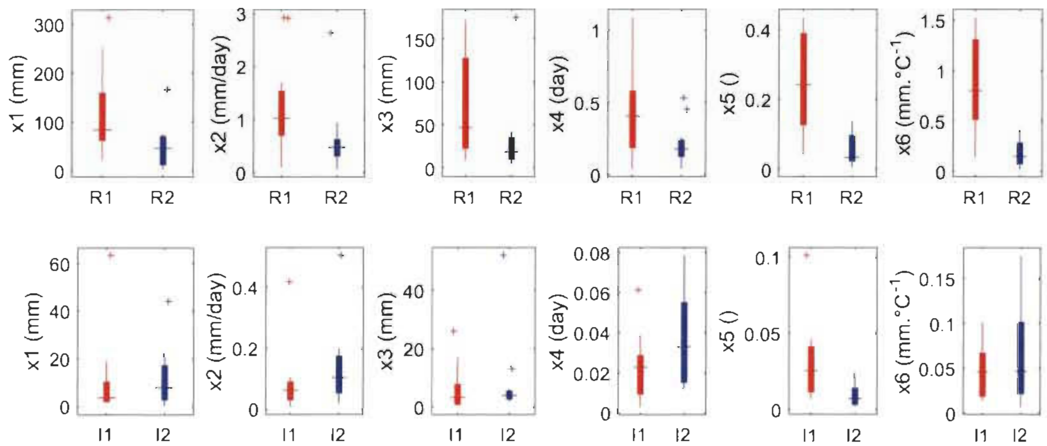

Fig. 8. Distribution of the range (R) and interquartile range (I) of equifinal parameter sets for the 12 basins and each of the six model parameters; R1: range for MULTI method (red); R2: range for SCE_Flow method (blue); I1: interquartile range for MULTI (red); I2: interquartile range for SCE_Flow (blue).

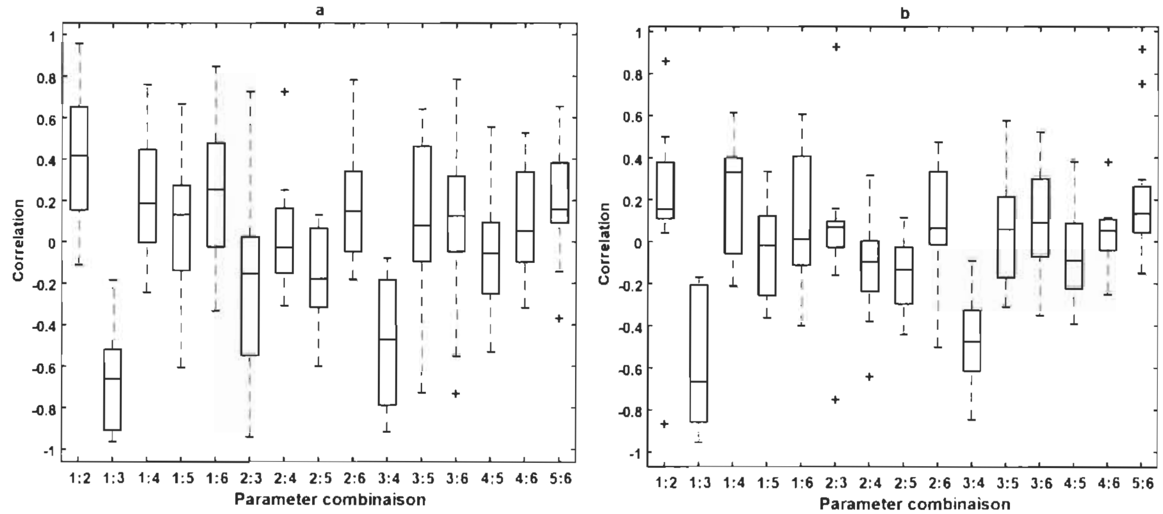

Fig. 9. Boxplots of Pearson correlation coefficients between parameter equifinal sets for the twelve basins: (a) SCE-FLOW; (b) MULTI.

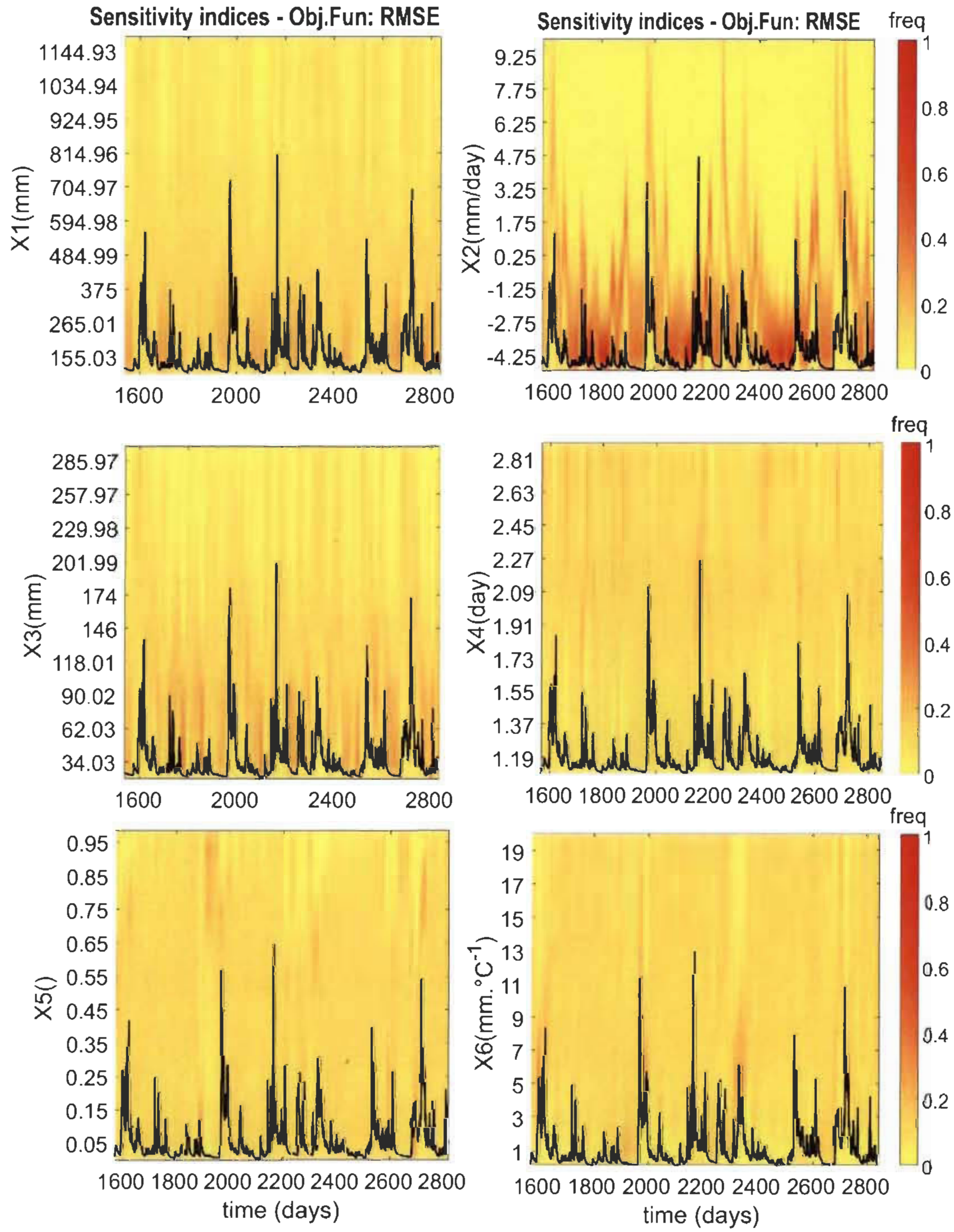

Fig. 10. Identifiability analysis of the six parameters of the GR4J-Cemaneige model by the DYNIA method (Wagener et al., 2003) RMSE computed over a moving window (15 days); the black line is the streamflow. A more reddish color indicates the zones, in the parameter space that give the 10% best simulations in the time window. The absence of a clear red zone means that all parameter values can give equally best simulation, i.e. the parameter is not identifiable.

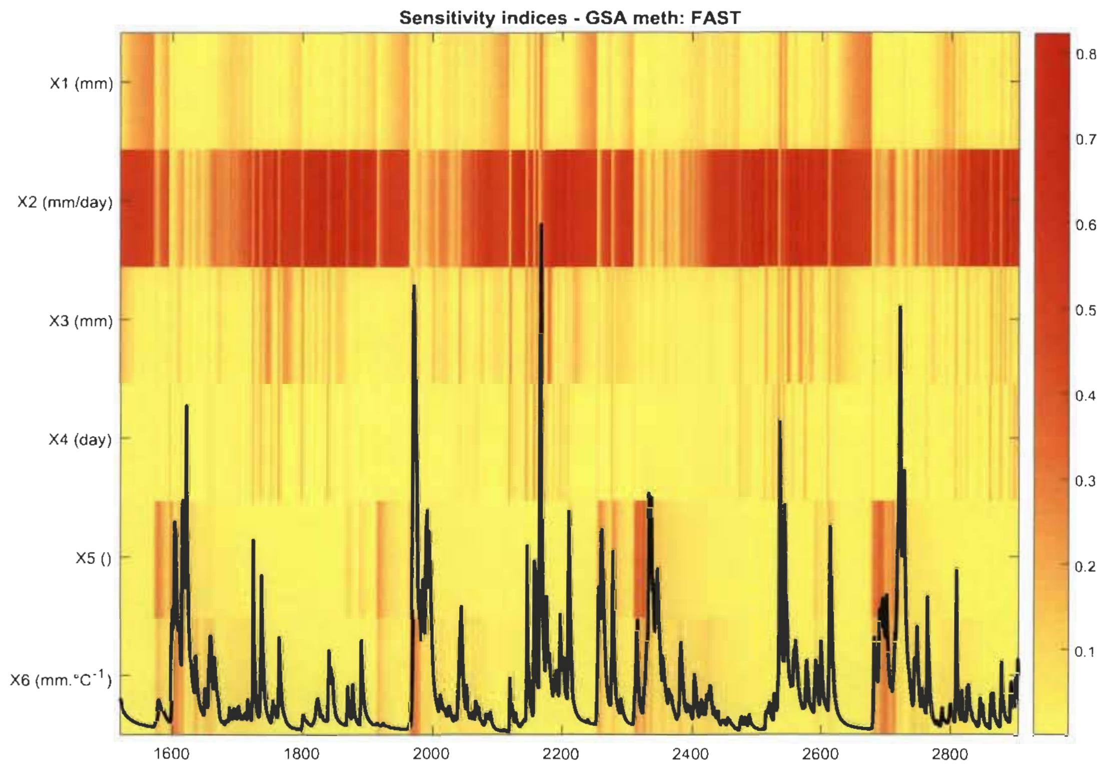

Fig. 11. Time-varying sensitivity analysis (TVSA) using global sensitivity analysis FAST indices (ranging from 0 to 1). A more reddish color indicates the most influential parameter.

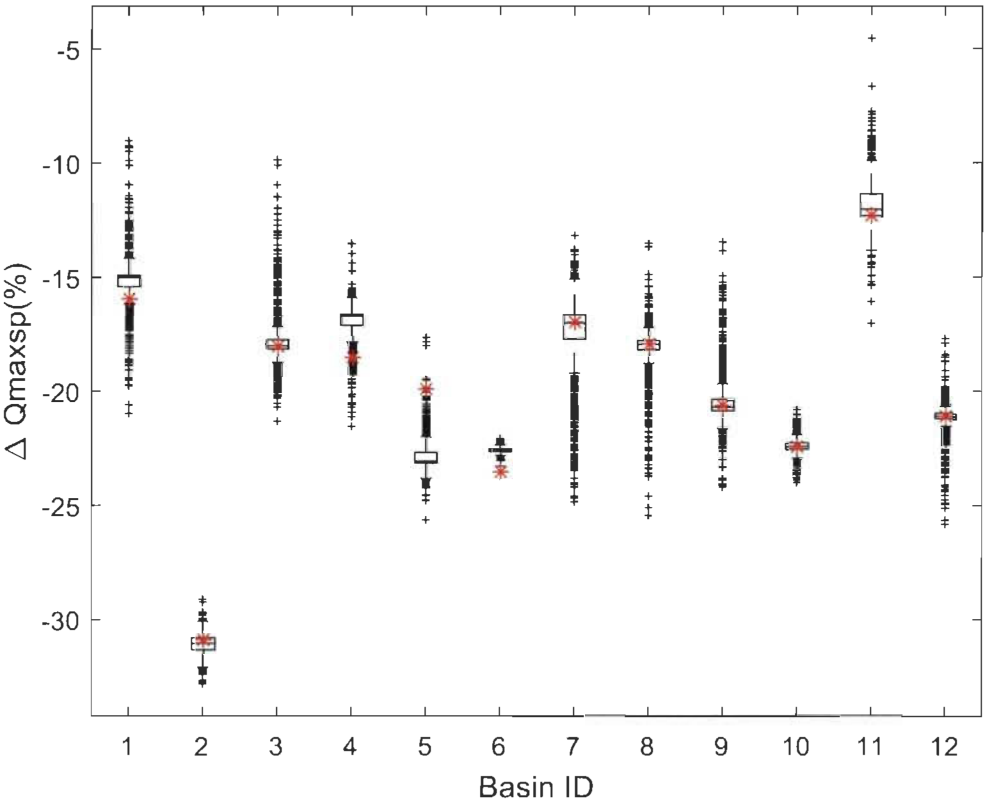

Fig. 12. Percent change in mean springtime peak streamflow $\Delta Qmax_{sp}$ in response to a +2 °C temperature perturbation for the 12 basins simulated with equifinal sets (boxplot) and the optimal set (red dot).

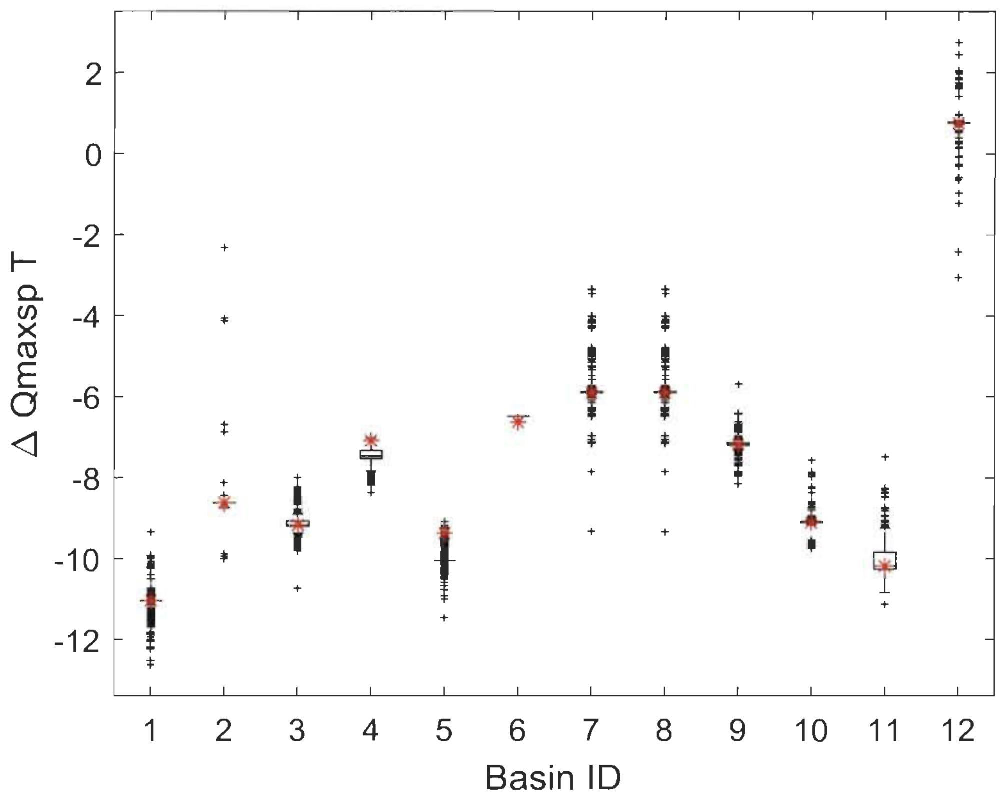

Fig. 13. Percent change in the timing of peak springtime streamflow $\Delta Qmax_{sp}T$ (days) for the 12 basins simulated with equifinal sets (boxplot) and optimal set (red dot) in response to a +2 °C temperature perturbation.

References

Andréassian, V., Moine, N. L., Perrin, C., Ramos, M.-H., Oudin, L., Mathevet, T., . . . Berthet, L. (2012). All that glitters is not gold: the case of calibrating hydrological models. *Hydrological processes, 26*, 2206-2210.

Arsenault, R. (2015). *Équifinalité, incertitude et procédures multi-modèle en prévision hydrologique aux sites non-jaugés.* Thèse de doctorat, École de technologie supérieure, Université du Québec.

Arsenault, R., & Brissette, F. P. (2014). Continuous streamflow prediction in ungauged basins: The effects of equifinality and parameter set selection on uncertainty in regionalization approaches. *Water Resources Research, 50*, 6135-6153.

Arsenault, R., Poulin, A., Côté, P., & Brissette, F. (2013). A comparison of stochastic optimization algorithms in hydrological model calibration. *Journal of hydrologic engineering*.

Bennett, K., Werner, A., & Schnorbus, M. (2012). Uncertainties in Hydrologic and Climate Change Impact Analyses in Headwater Basins of British Columbia. *American meteorological society*.

Bergeron, J., Royer, A., Turcotte, R., & Roy, A. (2014). Snow cover estimation using blended MODIS and AMSR-E data for improved watershed-scale spring streamfow simulation in Quebec, Canada. *Hydrological processes, 28*, 4626-4639.

Bergeron, O. (2015). *Grilles climatiques quotidiennes du Programme de surveillance du climat du Québec, version 1.2 – Guide d'utilisation*. Québec.

Beven, K. (2006). A manifesto for the equifinality thesis. *Journal of Hydrology 320*, 18-36.

Beven, K., & Freer, J. (2001). Equifinality, data assimilation, and uncertainty estimation in mechanistic modelling of complex environmental systems using the GLUE methodology. *Journal of Hydrology, 249*(1-4), 11-29.

Blasone, R. (2007). *Parameter estimation and uncertainty assessment in hydrological modelling.* Thesis, Institute of Environment & Resources Technical, University of Denmark.

Brigode, P., Oudin, L., & Perrin, C. (2013). Hydrological model parameter instability: A source of additional uncertainty in estimating the hydrological impacts of climate change? *Journal of Hydrology, 476*, 410-425.

Brown, R. D. (2010). Analysis of snow cover variability and change in Québec 1948-2005. *Hydrological processes, 24*, 1929-1954.

Chen, J., Brissette, F. P., Poulin, A., & Leconte, R. (2011). Overall uncertainty study of the hydrological impacts of climate change for a Canadian watershed. *Water Resources Research, 47*, W12509.

Coron, L., Andréassian, V., Perrin, C., Bourqui, M., & Hendrick, F. (2014). On the lack of robustness of hydrologic models regarding water balance simulation: a diagnostic approach applied to three models of increasing complexity on 20 mountainous catchments. *hydrology and Earth System Sciences, 18*, 727-746.

Coron, L., Andreassian, V., Perrin, C., Lerat, J., Vaze, J., Bourqui, M., & Hendrickx, F. (2012). Crash testing hydrological models in contrasted climate conditions: An experiment on 216 Australian catchments. *Water Resources Research, 48*, 17p.

Duan, Q., sorooshian, S., & Gupta, H. V. (1992). Effective and Efficient Global Optimization for Conceptual Rainfall-Runoff Models *Water Resources Research, 28*(4).

Duethmann, D., Peters, J., Blume, T., Vorogushyn, S., & G€untner, A. (2014). The value of satellite-derived snow cover images for calibrating a hydrological model in snow-dominated catchments in Central Asia. *Water Resources Research, 50*, 2002-2021.

Edijtano. (1991). Mise en point d'un modèle élémentaire Pluit-débit au pas de temps jounalier.

Efstratiadis, A., & Koutsoyiannis, D. (2010). One decade of multi-objective calibration approaches in hydrological modelling: a review. *Hydrological Sciences Journal, 55*(1), 58-78.

Fenicia, F., Savenije, H. H. G., Matgen, P., & Pfister, L. (2007). A comparison of alternative multiobjective calibration strategies for hydrological modeling. *Water Resources Research, 43*, W03434.

Ficklin, D., & Barnhart, B. (2014). SWAT hydrologic model parameter uncertainty and its implications for hydroclimatic projections in snowmelt-dependent watersheds. *Journal of Hydrology, 519*, 2081-2090.

Finger, D., Pellicciotti, F., Konz, M., Rimkus, S., & Burlando, P. (2011). The value of glacier mass balance, satellite snow cover images, and hourly discharge for improving the performance of a physically based distributed hydrological model. *Water Resources Research, 47*, W07519.

Foulon, É., & Rousseau, A. N. (2018). Equifinality and automatic calibration: What is the impact of hypothesizing an optimal parameter set on modelled hydrological processes? *Revue canadienne des ressources hydriques, 43*, 47-67.

Gupta, H. V., Bastidas, L. A., Vrugt, J. A., & Sorooshian, S. (2003a). Multiple Criteria Global Optimization for Watershed Model Calibration. In Q. Duan, H. V. Gupta, S. Sorooshian, A. N. Rousseau & R. Turcotte (Eds.), Calibration of Watershed Models. Washington: American Geophysical Union.

Gupta, H. V., Beven, K. J., & Wagener, T. (2006). Model Calibration and Uncertainty Estimation. *Encyclopedia of Hydrological Sciences, 138.*

Gupta, H. V., & Nearing, G. S. (2014). Debates – The future of hydrological sciences: A (common) path forward? Using models and data to learn: A systems theoretic perspective on the future of hydrological science. *Water Resources Research, 50*, 5351-5359.

Gupta, H. V., Sorooshian, S., Hogue, T. S., & Boyle, D. P. (2003b). Advances in Automatic Calibration of Watershed Models. In Q. Duan, H. V. Gupta, S. Sorooshian, A. N. Rousseau & R. Turcotte (Eds.), Calibration of Watershed Models Washington: American Geophysical Union.

Gupta, H. V., Sorooshian, S., & Yapo, P. O. (1998). Toward improved calibration of hydrologic models: Multiple and noncommensurable measures of information *Water Resources Research, 34*(4), 751-763.

Her, Y., & Seong, C. (2018). Responses of hydrological model equifinality, uncertainty, and performance to multi-objective parameter calibration. *Journal of Hydroinformatics, 20*(4), 864-885.

Her, Y., Yoo, S.-H., Seong, C., Jeong, J., Cho, J., & Hwang, S. (2016). Comparison of uncertainty in multi-parameter and multi-model ensemble hydrologic analysis of climate change. *Hydrology and Earth System Sciences, 160.*

Hogue, T. S., Gupta, H. V., Sorooshian, S., & Tomkins, C. D. (2003). A Multi-Step AutomaticC alibrationS chemef or WatershedM odels. In Q. Duan, H. V. Gupta, S. Sorooshian, A. N. Rousseau & R. Turcotte (Eds.), Calibration of Watershed Models. Washington: American Geophysical Union.

Jiang, T., Chen, Y. D., Xu, C.-y., Chen, X., Chen, X., & Singh, V. P. (2007). Comparison of hydrological impacts of climate change simulated by six hydrological models in the Dongjiang Basin, South China. *Journal of Hydrology, 336*, 316-333.

Kavetski, D., & Clark, M. P. (2011). Numerical troubles in conceptual hydrology: Approximations, absurdities and impact on hypothesis testing. *Hydrological processes, 25*(661-670).

Kay, A., Davies, H., Bell, V., & Jones, R. (2009). Comparison of uncertainty sources for climate change impacts: flood frequency in England. *Climatic Change, 63*, 92-41.

Klemes, V. (1986). Operational testing of hydrological simulation models. *Hydrological Sciences Journal, 31*(1), 13-24. doi: 10.1080/02626668609491024

Lay, M. L. (2006). *Modélisation hydrologique dans un coontexte de variabilité hydro-climatique. Une approche comparative pour l'étude du cycle hydrologique à méso-échelle au Bénin.* Institut National Polytechnique de Grenoble.

Madsen, H. (2003). Parameter estimation in distributed hydrological catchment modelling using automatic calibration with multiple objectives. *Advances in Water Resources, 26*, 205-216.

Merz, R., Parajka, J., & Blöschl, G. (2011). Time stability of catchment model parameters : Implications for climate impact analyses. *Water Resources Research, 47*.

Moradkhani, H., & Sorooshian, S. (2009). General Review of Rainfall-Runoff Modeling: Model Calibration, Data Assimilation, and Uncertainty Analysis. *Hydrological Modelling and the Water Cycle*, 1-24.

Nascimento, N. D. O. (1995). *Appréciation à l'aide d'un modèle empirique des effets d'actions anthropiques sur la relation pluie-débit à l'échelle d'un bassin versant.*

Parajka, J., & Blöschl, G. (2008). The value of MODIS snow cover data in validating and calibrating conceptual hydrologic models. *Journal of Hydrology 358*(3-4), 240-258.

Parajka, J., Merz, R., & Blöschl, G. (2007). Uncertainty and multiple objective calibration in regional water balance modelling: case study in 320 Austrian catchments. *Hydrological processes, 21*, 435-446.

Perrin, C. (2000). *Vers une amélioration d'un modèle global pluie-débit au travers d'une approche comparative.* Thèse de doctorat, Institut National Polytechnique de Grenoble.

Perrin, C., Michel, C., & Andreassian, V. (2003). Improvement of a parsimonious model for streamflow simulation. *Journal of Hydrology, 279*.

Perrin, C., Michel, C., & Andréassian, V. (2007). Modèles hydrologiques du Génie Rural (GR): Cemagref, UR Hydrosystèmes et Bioprocédés.

Pianosi, F., & Wagener, T. (2016). Understanding the time-varying importance of different uncertainty sources in hydrological modelling using global sensitivity analysis. *Hydrological processes, 30*, 3991-4003.

Poirier, C., Filion, T. C. F., Turcotte, R., & Lacombe, P. (2014). Reconstitution historique des apports verticaux (eaux de fonte et de pluie) de 1900 à 2010, version 2012. Contribution au Programme d'acquisition de connaissances sur les eaux souterraines (PACES) (pp. 99) : Centre d'expertise hydrique du Québec (CEHQ).

Poulin, A., Brissette, F., Leconte, R., Arsenault, R., & Malo, J.-S. (2011). Uncertainty of hydrological modelling in climate change impact studies in a Canadian, snow-dominated river basin. *Journal of Hydrology, 409*, 626-636.

Reusser, D., & Zehe, E. (2011). Inferring model structural deficits by analyzing temporal dynamics of model performance and parameter sensitivity. *Water Resources Research, 47.*

Roy, A., Royer, A., & Turcotte, R. (2010). Improvement of springtime streamflow simulations in a boreal environment by incorporating snow-covered area derived from remote sensing data. *Journal of Hydrology, 390*, 35-44.

Seiller, G., & Anctil, F. (2014). Climate change impacts on the hydrologic regime of a Canadian river: comparing uncertainties arising from climate natural variability and lumped hydrological model structures. *Hydrology and Earth System Sciences, 18*, 2033-2047.

Seiller, G., Anctil, F., & Perrin, C. (2012). Multimodel evaluation of twenty lumped hydrological models under contrasted climate conditions. *Hydrology and Earth System Sciences, 16*, 1171-1189.

Sena, N., Chokmani, K., Gloaguen, E., & Bernier, M. (2016). Analyse multi-échelles de la variabilité spatiale de l'équivalent en eau de la neige (EEN) sur le territoire de l'Est du Canada. *Hydrological Sciences Journal*, 1-16.

Shin, M.-J., Guillaume, J. H. A., Croke, B. F. W., & Jakeman, A. J. (2015). A review of foundational methods for checking the structural identifiability of models: Results for rainfall-runoff. *Journal of Hydrology, 520.*

Tang, Y., Reed, P., & Wagener, T. (2006). How effective and efficient are multiobjective evolutionary algorithms at hydrologic model calibration? *Hydrology and Earth System Sciences, 10*, 289-307.

Teng, J., Vaze, J., Chiew, F., Wang, B., & Perraud, J.-M. (2011). Estimating the Relative Uncertainties Sourced from GCMs and Hydrological Models in Modeling Climate Change Impact on Runoff. *Journal of Hydrometeorology*.

Troin, M., Arsenault, R., & Brissette, F. (2015). Performance and Uncertainty Evaluation of Snow Models on Snowmelt Flow Simulations over a Nordic Catchment (Mistassibi, Canada). *Hydrology 2*, 289-317.

Turcotte, R. (2010). *Éléments du calage et de l'implantation d'un modèle hydrologique dans une perspective d'utilisation opérationnelle en prévision hydrologique.* Thèse de doctorat, Université du Québec.

Turcotte, R., Filion, T.-C. F., Lacombe, P., Fortin, V., Roy, A., & Royer, A. (2010). Simulation hydrologique des derniers jours de la crue de printemps : le problème de la neige manquante. *Hydrological Sciences Journal, 55*(6), 872-882.

Turcotte, R., Fortin, L.-G., Fortin, V., Fortin, J.-P., JeanPierre, Villeneuve, & (2007). Operational analysis of the spatial distribution and the temporal evolution of the snowpack water equivalent in southern Québec, Canada *Hydrology Research, 38*(3), 211-234.

Turcotte, R., Rousseau, A. N., Fortin, J.-P., & Villeneuve, J.-P. (2003). A Process-Oriented, Multiple-Objective Calibration Strategy Accounting for Model Structure. In Q. Duan, H. V. Gupta, S. Sorooshian, A. N. Rousseau & R. Turcotte (Eds.), Calibration of Watershed Models. Washington: American Geophysical Union.

Udnæs, H.-C., Alfnes, E., & Andreassen, L. M. (2007). Improving runoff modelling using satellite-derived snow covered area? *Hydrology Research, 38*(1), 21-32.

Valéry, A. (2010). *Modélisation précipitations – débit sous influence nivale: Elaboration d'un module neige et évaluation sur 380 bassins versants.* Thèse de doctorat, AgroParisTech, Paris.

Valéry, A., Andréassian, V., & Perrin, C. (2014a). 'As simple as possible but not simpler': What is useful in a temperature-based snow-accounting routine? Part 1 – Comparison of six snow accounting routines on 380 catchments. *Journal of Hydrology, 514*, 1166-1175.

Valéry, A., Andréassian, V., & Perrin, C. (2014b). 'As simple as possible but not simpler': What is useful in a temperature-based snow-accounting routine? Part 2 – Sensitivity analysis of the Cemaneige snow accounting routine on 380 catchments. *Journal of Hydrology, 517*, 1176-1187.

Vos, N. J. d., Rientjes, T. H. M., & Gupta, H. V. (2010). Diagnostic evaluation of conceptual rainfall–runoff models using temporal clustering. *Hydrological processes, 24*, 2840-2850.

Vrugt, J. A., & Robinson, B. A. (2007). *Improved evolutionary optimization from genetically adaptive multimethod search.* Paper presented at the Proceedings of the National Academy of Sciences of the United States of America.

Wagener, T., & Gupta, H. V. (2005). Model identification for hydrological forecasting under uncertainty. *Stochastic Environmental Research and Risk Assessment, 19*, 378-387.

Wagener, T., McIntyre, N., Lees, M. J., Wheater, H., & Gupta, H. V. (2003). Towards reduced uncertainty in conceptual rainfall-runoff modelling: Dynamic identifiability analysis. *Hydrological processes, 17*, 455-476.

Wilby. (2005). Uncertainty in water resource model parameters used for climate change impact assessment. *Hydrological processes, 19*, 3201-3219.

Wilby, & Harris, I. (2006). A framework for assessing uncertainties in climate change impacts: Low-flow scenarios for the River Thames, UK. *Water Resources Research, 42*.

Yapo, P. O., Gupta, H. V., & Sorooshian, S. (1998). Multi-objective global optimization for hydrologic models. *Journal of Hydrology, 204*, 83-97.

CHAPITRE III

MECHANISMS OF SPRING FRESHET GENERATION IN SOUTHERN QUEBEC, CANADA

Article en attente de soumission au journal scientifique *Hydrological Processes*

Saida Nemri[1], Christophe Kinnard[1]

[1] Département des Sciences de l'environnement, Université du Québec à Trois-Rivières, C. P. 500, Trois-Rivières, Québec, G9A 5H7 Canada

Corresponding author: Christophe Kinnard

E-mail: Christophe.Kinnard@uqtr.ca

Abstract

Seasonal forecasting of spring floods in snow-covered basins is still difficult and uncertain due to the ambiguity in the driving processes, errors in the initial conditions and the choice of predictor variables. In this study we attempt to improve the prediction of spring flow peaks in southern Quebec, Canada, by studying the preconditioning mechanisms of runoff generation and their impact on inter-annual variations in the timing and magnitude of spring peak flow. Historical observations and simulated data from a hydrological and snowmelt model are used to study the antecedent conditions that control flood characteristics in twelve snow-dominated catchments. Over a pre-flood period extending from the onset date to the spring peak flow, the relative contributions of snowmelt, rainfall, melt intensity, rainfall intensity and soil moisture in driving interannual changes in spring peak flow were assessed. A multivariate linear regression analysis was used to predict the magnitude and timing of the spring peak flow using the hydrological antecedent factors as predictors. Results show that interannual variations in spring peak flow are controlled differently between basins. Overall interannual variations are mainly explained, in order of importance, by melt intensity, rain intensity, melt volume, total rainfall, peak SWE at the beginning of spring, and soil moisture. Variations in the timing of peak flow are controlled in most basins by total rainfall and rainfall intensity. In the northernmost, snow-dominated basins rain amount and intensity mostly control flow peaks variations, whereas for the southern, rainier basins snowpack conditions control this variability. Also, as melting is more gradual in the more forested basins, snowpack interannual variations are less important than variations in rain. On the other hand, in more agricultural basins melting is naturally faster and as such variations in snowpack conditions have a larger influence on the variability of spring flow peaks.

Keywords: spring freshet; runoff generation; spring floods; snowmelt intensity; rain-on-snow.

Introduction

The hydrology of cold regions is characterized by long winters dominated by snowfall and rapid spring melting which is the main cause of the high spring streamflow (Buttle et al., 2016; Pomeroy et al., 2016). In the province of Quebec, Canada, the amount of accumulated snow is very important, with a mean annual maximum of 200 to 300 mm of snow water equivalent (SWE) (Brown, 2010). The streamflow regime is nival to nivo-pluvial and strongly influenced by the snowmelt contribution, which occurs between April and June depending on the basin geographic location and the year. In the southern basins snow begins to accumulate in November and melting occurs between March and May. Peak flow is typically recorded in the spring following the melt and a second peak occurs in summer in response to convective rainstorms, or in the fall caused by the advection of moist air masses with above-freezing temperatures. In northern Quebec, snow accumulation begins earlier in October and melting occurs later in June and July with a single streamflow peak being observed, mainly caused by snowmelt (Assani et al., 2010; Buttle et al., 2016; Saint-Laurent et al., 2009). Hence knowledge of the SWE stored in the winter snowpack and of ablation dynamics in the spring is key for accurate streamflow predictions and operational management of reservoirs in Quebec. As such, a reliable seasonal forecast of spring freshet based on winter and early spring conditions is essential for reservoir operators to optimize two conflicting objectives, namely flood protection and hydropower production (Turcotte et al., 2010). Nevertheless, the relation between snow conditions and the inter-annual variations in the magnitude and timing of the spring peak flow is not straightforward, due to the complexity of spring runoff generation mechanisms. In fact, the same annual snow accumulation can induce more or less severe floods because of the multiplicity of antecedent hydrological conditions that can control runoff in addition to snow, such as meteorological conditions during the melt period, the occurrence of rain-on-snow events, and soil moisture. Therefore, a good understanding of the flood generation mechanisms and of the relative contribution of the key driving factors involved is essential to explain the interannual variability of the spring peak flow characteristics and guide future forecasting efforts.

The variability in flood characteristics in North America has been linked with large-scale climatic indices, and several previous studies have studied how these indices influence extreme floods (Assani et al., 2010; Assani et al., 2010b). Mazouz et al. (2013) studied the relationship between the interannual variations of high spring flow characteristics in southern Quebec (magnitude, duration, period of occurrence, frequency, and variability) and several global climatic indices using canonical correlation analysis. A significant correlation between the Atlantic Multi-Decadal Oscillation (AMO) and North Atlantic Oscillation (NAO) indices and four flood characteristics (duration, period of occurrence, frequency, and variability) was found while no relationship was found between these indices and the flow magnitude. This correlation was explained by the low temperature during the negative phases of the AMO and the positive phases of the NAO, which causes a later date of occurrence, a higher frequency, a longer duration and lower variability of heavy spring floods (Mazouz et al., 2013). Additionally, heavy rainfall events during spring may accelerate snowmelt and cause more devastating floods (Fang et al., 2016; Pomeroy et al., 2016; Sui et al., 2001) depending on the antecedent conditions of the snowpack (Garvelmann et al., 2015). During these events, the relative contribution of melting and rainfall becomes more complicated and affects the results of forecasting studies. This phenomenon of rain-on-snow in Canada has been addressed by several authors (Dyer, 2008; Mccabe et al., 2007; Pomeroy et al., 2016; Wayand et al., 2015). In Quebec, many devastating spring floods have been caused by a combination of heavy rainfall during melting and a deep accumulated snowpack, such as for the Richelieu river floods in 2011 (Saad et al., 2015). Teufel et al. (2018) studied the devastating spring floods that occurred in Montreal during May 2017, showing that heavy rainfall events during April and May and snowmelt were the culprit of these extreme events. Likewise, moisture state of the catchment plays a key role in runoff generation during melt. In fact, the degree of soil saturation below the snowpack determines the infiltration and the runoff of snowmelt water in snow-covered basins (Koster et al., 2010; Mahanama et al., 2012). These two studies have quantified the contributions of snow accumulated on January 1st and soil moisture to the skill of seasonal forecast of spring snowmelt in 23 basins of the eastern United States. They demonstrated that despite the important role of snow, the contribution of soil moisture in the skill of streamflow forecast is significant. Several studies showed also the importance of 'soil memory', i.e. soil moisture conditions before soil freezing (Curry et al., 2017; Mahanama et al., 2012; Webb et al., 2018; Wever et al., 2017) so that understanding the relationship between floods, soil moisture and snow cover in these basins is necessary to understand the spring streamflow generation.

The main challenges in studying how antecedent hydrological variables control spring floods are the choice of predictors, the interaction between them, the period over which these factors will be calculated and the unavailability of observations for some factors such as soil moisture and SWE (Coles et al., 2016; Curry et al., 2017; Fang et al., 2016; Nied et al., 2013; Nied et al., 2014). In western Canada, Curry et al. (2017) investigated the influence of a set of factors on the variability of annual maximum daily flow magnitude using multivariate linear regression models in a snow-dominated basin. They ranked the effect of a set of predictors according to their degree of control on the maximum basin peak flow as follows: the maximum annual snowpack (SWEmax), the melting rate calculated between SWEmax and peak flow, the Pacific Decadal Oscillation (PDO) and El Niño-Southern Oscillation (ENSO), and finally the rate of warming calculated between April 1st and the date of peak flow. Some variables used were measured while others were simulated by a hydrological model, such as the melt rate and soil moisture. Coles et al. (2016) studied snowmelt runoff generation in the Canadian prairies hillslopes using a decision tree learning approach to rank the processes responsible for the generation of runoff. The impact of variables on flow peak, in order of importance, were as follows: total snowfall, snow cover, fall soil surface water content, melt rate, melt season length, and fall soil profile water content. Among its most important results was the importance of the degree of soil saturation during the fall before the frost period, or soil memory, in controlling runoff. Fang et al. (2016) studied the sensitivity of the June 2013 flood in Calgary to pre-flood conditions as simulated by the physically-based hydrological model CRHM. They studied streamflow generation processes by varying the amount of precipitation, the land cover and soil storage capacity during the pre-flood period. It was shown that runoff increases rapidly in response to prior accumulation of snow and soil moisture and that antecedent soil moisture in the basin is a better indicator of flood magnitude than the antecedent snowpack in this basin.

In Quebec basins, the hydrological drivers, or 'predictors' of interannual variations in the magnitude and timing of the spring flow peak are not well identified and have not been studied except in relation with global climatic indices (Assani et al., 2010a; Assani et al., 2010b; Mazouz et al., 2013). Hence the main objective of this study is to identify and better understand the factors that control the variation of spring freshet characteristics in the catchments of the St. Lawrence tributaries in order to improve seasonal forecasts. The limited availability of snow depth, snow water equivalent (SWE) and soil moisture observations has always been an obstacle when analyzing historical hydrological datasets. In this study, we use outputs of simplified conceptual models to simulate snow accumulation and melt as well as soil moisture storage in the basins. We seek to answer the following questions: (i) is the inter-annual variability in the magnitude of the spring freshet peak mainly dependent on the antecedent snowpack, so that higher flow peak occurs in years with deep snowpack? (ii) Does the quantity and intensity of rainfall during the pre-flood period affect the characteristics of the spring freshet? (iii) How do the preconditioning factors vary between basins, according to their latitude and physiographic region?

Study Area and Data

This study was carried out on twelve tributary catchments of the St. Lawrence River located in the province of Quebec, Canada with a natural hydrological regime (Fig. 1). The area of the catchments varies between 367 and 4504 km^2 (Table 1). They are spatially distributed between the north and south shore of the St. Lawrence River and within four homogeneous hydrological regions used by the Quebec Center for Water Expertise (CEHQ) in charge of streamflow monitoring and forecasting. The Northwest St. Lawrence region (Batiscan, Bras du Nord, Matawin) is characterized by a continental climate; the Saint-Laurent Southwest region (Nicolet, Acadie) is characterized by a maritime climate; the Saint-Laurent Southeast region (York, Beaurivage, Bécancour, Famine, Etchemin, Ouelle) characterized by a mix of maritime and continental climate and Saint-Laurent Northeast region (Godbout) characterized by a maritime climate (Assani et al., 2010a; Assani et al., 2010b; Mazouz et al., 2013). These basins are located in three different physiographic regions: the St Lawrence Lowlands characterized by a flat relief (Acadie), the north shore of the St. Lawrence River in Canadian Shield forested lands (Batiscan, Matawin, Bras du Nord and Godbout); the remaining seven basins (Ouelle, York, Etchemin, Bécancour, Famine, and Nicolet) are located on the south shore of the St. Lawrence River in the Appalachian Mountains (Table 1).

The six basins Batiscan, Godbout, Matawin, Ouelle, York, Famine, and Bras du Nord are completely forested basins with approximately 90% of the area covered by forest and the remaining area covered by agriculture and lakes. The land cover in the Acadie basin is dominated by agriculture (72%) with only 25% covered by forest. The three basins Nicolet, Etchemin, and Bécancour have the same forest (70%) and agriculture (25%) cover (in Table 1).

Daily historical streamflow data at the outlet of the 12 basins were extracted from the website of the Quebec Center for Water Expertise (CEHQ) (www.cehq.qc.ca). The length of the observed data varies between basins, from 33 to 55 years. A method developed as part of this study, described in the next section, was used to separate spring streamflow using the daily observed flows.

Having a good estimation of pre-flood snowpack is one of the challenges to understand the contribution of snowmelt to peak flow variability. However, the difficulty of measuring snow depth and snow water equivalent (SWE) typically results in limited data being available, over time and space. Remote sensing tools are used to estimate the snow cover and the SWE in low vegetation areas but problems remain in forested areas (Bergeron et al., 2014; Brown, 2010; Sena et al., 2016). In Quebec, a network of snow survey sites has been installed in forested areas to measure the water equivalent of snow (SWE) and the depth of snow every two weeks in the winter and spring seasons, but the spatial distribution and density of these stations is low. Consequently, using outputs of hydrological models seems the only solution to derive long SWE and soil moisture records. In a previous study conducted in the same basins by Nemri and Kinnard (2019), The GR4J hydrological model coupled to the Cemaneige snow model has been calibrated and validated in order to properly simulate basin-wide SWE, soil moisture and daily streamflow. The calibration methods and validation results are well described in Nemri and Kinnard (2019). A multi-objective calibration strategy was found to give the best simulation of both streamflow and SWE, and the simulation results using this method were used in the present study. The model was forced by daily precipitation and temperature date extracted from daily grids produced by the Atmospheric Environment Information Service (SIMAT) in collaboration with the Quebec Center for Water Expertise (CEHQ) (Bergeron, 2015). Historical SWE measurements at 12 measuring points of the Quebec snow survey network located in or very close to the selected basins were used in the calibration along with the observed flow (see Fig. 1). Daily precipitation during the pre-flood period was separated in a rain and snowfall fraction based on air temperature. The snowmelt module Cemaneige Valéry (2010) simulates the accumulation and snowmelt in five altitude bands. The precipitation phase (rain, snow) is determined using the mean temperature of each altitude band, according to two methods depending on the median altitude of the basin. If the median altitude is higher than 1500 m the method developed by the US Army Corps of Engineers (1956) is used, in which the snow/rain fraction is interpolated between -1 °C (all snow) and 3 °C (all rain). If the median altitude is less than 1500 m, which is the case for all basins in this study, the fraction of snow is calculated according to the function used in the Hydrotel model (Fortin et al., 2001). The snow/rain fraction is estimated as a function of the minimum (T_{min}) and maximum (T_{max}) daily temperature of each altitude band: when $T_{max} \leq 0$ °C all precipitation fall as snow, while if $T_{min} \geq 0$ °C all precipitation fall as rain, else the snow fraction is estimated as $1\text{-}T_{min}/(T_{max}\text{-}\ T_{min})$. These functions are well described by Valéry (2010) and Valéry et al. (2014b). In addition, soil moisture measurement were not available for the study so that soil moisture simulated by the conceptual model GR4J was used. In GR4J the hydrological processes in the basin are simplified into two interconnected reservoirs. The soil reservoir has a maximum capacity (mm), which is a free parameter to be calibrated, and determines the amount of water in the basin according to the degree of soil saturation, itself a function of the ratio between the quantity of stored water and the maximum storage capacity.

Methodology

Spring flood identification

The first analysis step was to identify the pre-flood factors and the period over which to calculate them. A sufficiently large spring window of four months, from March 1st to June 30th, was selected based on daily observed streamflow and taking into account the inter-annual and spatial variability of the spring freshet of all basins. The maximal daily flow value and its timing observed within this time window were identified for every year. Then, the pre-flood period was set between the flood onset point, defined here as the point that marks the beginning of the rise in streamflow, and the peak flow date (Fig. 2). The onset point was identified as the first point having a flow value above the 30% percentile of the annual flow distribution and followed by a continuous increase in flow over a minimum of three consecutive days, before the peakflow date. This automatic procedure worked well for most years and basins, but exceptions were noted upon visual inspection. Hence for some years the percentile threshold was either adjusted, or the point was chosen manually when the automatic algorithm failed. Identifying the spring flood onset date was difficult when the form of the hydrograph was irregular, i.e. for complex, multiple-peak floods. In fact, snowmelt is discontinuous in several years. This intermittent snowmelt is due to low air temperatures associated with the advection of cold polar air masses which stops snowmelt for days and causes separate floods according to melting events (Mazouz et al., 2013). This makes it difficult in some years to precisely pinpoint a general flood onset date and this decision may subsequently influence the relation between the peak flow magnitude and the pre-event variables.

Antecedent factors and statistical analysis of spring freshet peak

The objective is to understand if the interannual variability in the timing and magnitude of the spring streamflow peaks depends mainly on the amount of accumulated snow and its rate of melting, and what is the effect of antecedent soil saturation conditions and rainfall events during melting. Hence two spring streamflow characteristics, the magnitude *Qmax* and timing of peak flow (in day of year or DOY) *Qmax_T* were selected to characterize the spring freshet, and their interannual variability calculated from the daily flow historical records. In total, six antecedent factors related to snowmelt, rainfall and soil moisture were selected and calculated during the pre-flood period as defined in section 3.1., except for the annual maximum snowpack (peak SWE) which was calculated over the entire hydrological year. The daily pre-flood variables were computed taking into account the time of transfer of the basin, i.e. preconditioning variables were calculated from the flood onset date up to x4 days before the flood peak date calibrated for each basins, where x4 is the base time of the unit hydrograph in the GR4J hydrological model and was calibrated by Nemri and Kinnard (2019). The Cemaneige model simulates snow accumulation and melt in five altitudinal bands and extrapolates the meteorological data (temperature, precipitations) according to the median altitude of the band. However, all variables used here are the mean of the basin and not related to a specific band. The contribution of snowpack conditions to the variations in spring peak flow characteristics, *Qmax* and *Qmax_T*, was assessed by three variables: (i) the maximum SWE, *Gmax* (mm), simulated by the model before the melt, between the beginnings of spring (March 1) and the peak flow date, represents the amount of snow accumulated and to be released during the spring freshet. A good correlation between *Gmax* and maximum streamflow would imply that *Gmax* is good predictor that can ameliorate seasonal flood forecasts. The quantity of snowmelt and its rate of melting are also used to evaluate their contribution to interannual variability in peak flow characteristics. The sum of the pre-flood melting, *Melt_sum* (mm), was simulated by Cemaneige and the melt intensity *Melt_int* (mm/d) is the melting rate calculated as the mean over the pre-event period. Rainfall is used as another antecedent condition that can affect streamflow in this period by changing snowpack characteristics or directly contribution to runoff. The sum of daily rain, *Rain_sum* (mm), accumulated during the pre-flood period, was calculated after separating the solid and liquid fraction in the snow model, and the mean rain intensity, *Rain_Int* (mm/d), are selected as potential predictors. The mean soil moisture saturation level during the pre-flood period, *Smean* (unitless), was simulated by the model and used as another antecedent factor. The selected antecedent factors are summarized in Table 2.

The relationship between the antecedent factors and peak streamflow characteristics was assessed initially by linear univariate correlation analysis using the Pearson correlation coefficient. Following this, a stepwise multivariate regression analysis was performed (Equation 1).

$$Y = \beta 0 + \beta 1 X1 + \beta 2 X2 + \cdots + \beta n Xn \qquad \text{Equation (1)}$$

where $\beta 0$ is the intercept and $\beta 1 \ldots n$ are the regression slope coefficients. The stepwise method consists in choosing the combination of pre-flood predictor variables (X) which together best explain the characteristics of floods (response variables Y) using an iterative procedure. The stepwise procedure requires two significance levels for adding and removing predictors based on a variance ratio (F) test, for the improvement of the model. Starting with the initial model, a *p*-value for the F-statistic is calculated at each step of adding or removing a variable in the model. An entrance tolerance *p*-value of < 0.05 and an exit tolerance *p*-value < 0.1 were used.

Results

Inter-annual and spatial variability of peak streamflow and its date of occurrence

The variability of the spring streamflow magnitude *Qmax* observed in the twelve basins, sorted by latitude from south to north, is shown in Fig. 3a. The highest median *Qmax* values are observed in the basins Batiscan, Bécancour, Nicolet, and Godbout which are the largest basins (cf. Table 1). Boxplots show that the peak streamflow is also more variable between years in these basins. The smallest *Qmax* value is recorded in the smallest basin Acadie (ID#1). The month of occurrence of spring maximum flow is shown in Table 2. For the two northernmost basins, i.e. Godbout and York, 90% of the flow peaks occurs the latest, in the month of May. For the two southernmost basins, i.e. Nicolet and Acadie, melting occurs earlier with 40% of peakflow events occurring in March and 40% in April. For the remaining basins, 65% of the peakflow events occur during April. Fig. 3b shows the high inter-annual variability of the peakflow timing in terms of day of the year (DOY), and also the spatial variability between the basins. The general increasing trend from south to north in the peakflow timing also appears clearly. Also, for the three completely forested basins located in the Canadian Shield, i.e. Batiscan (#5), Matawin (#7) and Bras du Nord (#9) melting occurs later compared to basins at the same latitude with less forested area such as Beaurivage (#6: 60%) and Etchemin (#8: 74%). Therefore, the spatial distribution of the *Qmax* timing is seen to primarily be a function of latitude and land cover.

Contribution of melt and rain to flood volumes

The contribution of pre-flood vertical inflows (melt and rain) volumes to the total flood volume calculated during the pre-flood period is illustrated in Fig. 4 for the twelve basins. The boxplots in Fig. 4a show the volume of snowmelt and rain during the pre-flood period for each basin while the corresponding contributing fraction to the total flood volume is shown in Fig. 4b. It is very clear for the southernmost Acadie basin that the rain contribution is high compared to the other basins. While the median rain contribution (0.25) is only slightly higher than that of other basins, the interannual variability is large, with the third quartile of the distribution reaching near 0.75, and in some extreme years rain was the sole contributor. For the other basins, the median rain contribution is around 0.2, but the fraction can be as high as 0.6, which shows that the rain contribution to the spring flood volume in all basins can be important. Multivariate linear regression analysis was conducted to study how interannual variations in rainfall and snowmelt volumes explain the variability in total spring flood volume. Variations in vertical inflow (melt and rain) volumes explain between 67% and 93% of the interannual variability in peak volumes (Table 5). For the five southern basins located on the north shore of the St. Lawrence River, in the Canadian Shield forest (Nicolet, Acadie, Batiscan, Matawin and Bras du Nord), the effect of rain and snowmelt variability on streamflow volume is comparable, whereas for the other seven basins the interannual variability in flood volume is more controlled by snowmelt volume than rainfall.

Correlation between antecedent factors and spring flow peak and timing

The Pearson's linear correlation coefficient was first used to assess the significance of correlation ($p < 0.05$) between observed streamflow characteristics (*Qmax* and *Qmax_T*) and the antecedent factors. Correlations between *Qmax* and the six factors for the 12 basins are displayed on a correlogram (Fig. 5). Melt intensity *Melt_int* is positively correlated with the flow magnitude in all basins; the correlation is significant ($p < 0.05$) in most basins, with a Pearson correlation coefficient between 0.37 and 0.75, except for the three basins Bras du Nord, Bécancour and Batiscan. The simulated spring peak SWE (*Gmax*) also stands out as a good predictor of *Qmax* with a positive correlation found in all basins; significant correlations between 0.31 and 0.53 are found in all basins except Bras du Nord, Bécancour, Beaurivage, and Ouelle. Thus, years with higher snow accumulation and higher melting rate (intensity) generally tend to result in higher peak flow. The sum of snowmelt simulated during the pre-flood period *Melt_sum* is positively and significantly correlated with *Qmax* in only five basins. The accumulated rainfall events before peakflow and their intensity do not show any significant univariate relation with spring *Qmax*, except for the two basins Matawin and Godbout where *Qmax* is positively correlated with rainfall intensity (*Rain_int*). Soil moisture *Smean* is significantly and positively correlated with *Qmax* in only three basins (Batiscan, Famine and Matawin) and negatively correlated in Bécancour. In the basins Bécancour and Bras du Nord, *Qmax* is not correlated with peak SWE nor with variables related to snow melting *Melt_int* and *Meltsum*, which is not logical for these basins with a nival regime.

The correlation coefficient of *Melt_int* is stronger than for *Gmax* in six basins, while *Gmax* is a better predictor in only two basins, Nicolet and York. Overall, the correlation analysis shows that the pre-flood melt intensity *Melt_int* is the best overall predictor of the maximum spring streamflow variability, followed by the maximum SWE accumulated in winter *Gmax,* which is logical given the strongly nival character of the hydrological regime of rivers in Quebec. On the other hand, the correlation coefficients are overall only moderate, therefore a combination of several factors could better explain the variability in spring flow magnitude.

For the peakflow timing the pre-flood rainfall sum significantly controls *Qmax_T* in all basins, except for the three basins Famine, Acadie, and Godbout (Fig. 6). This means that in years with high rainfall volumes during the pre-flood period the streamflow peak occurs later. Melting intensity is significantly anti-correlated with *Qmax* timing in all but four basins, with correlations varying between -0.31 and -0.56, so when melting is rapid peakflow occurs earlier. The correlation with soil moisture is not spatially coherent, being significantly anti-correlated with flow timing in three basins (Acadie, Famine, and Beaurivage) and positively correlated in Batiscan, Matawin, Bras du Nord, Godbout, and Etchemin.

Multivariate regression

Interannual changes in spring *Qmax* can be induced by a combination of factors. For example, the same snowpack can result in different peakflow magnitudes if it is accentuated by abnormal rainfall events, rapid melt due to high spring warming rate or saturated soil before melting. The combination of pre-flood factors which best explain the inter-annual variations in maximum spring streamflow and its date of occurrence was thus assessed by stepwise multivariate linear regression. The multivariate linear regression models found differ between basins (Table 6). In fact, in only five basins (Acadie, Bécancour, Famine, Matawin and Etchemin) do the linear model explains more than 35% of *Qmax* inter-annual variations (adjusted $R^2 > 0.35$). For the remaining seven basins (Nicolet, York, Beaurivage, Bras du Nord, Batiscan and Godbout) the linear models only explain up to 30% of the variability of *Qmax*.

The snowmelt intensity *Melt_int* was the only significant predictor kept by the stepwise analysis to explain *Qmax* in three basins (Acadie, Godbout, and Beaurivage). In the southernmost Acadie basin melt intensity explains 60% of the variations in *Qmax* ($R^2 = 0.6$). In Godbout, which is located further north, only 20% of *Qmax* variations are explained by *Melt_int* even thought the correlation analysis also showed a significant correlation of *Qmax* with *Rain_int* and *Gmax,* but these variables were excluded from the variable selection stepwise method, which mean they did not bring any additional significant prediction skill. The same occurs for the Beaurivage basin where melt intensity only explained 10% of *Qmax* variations. The peak SWE *Gmax* is the only predictor retained for the two basins Nicolet and York and only explained 20% of *Qmax* in the southern Nicolet basin, even if *Melt_int* was also found to be significantly correlated, which means that this variable did not improve model skill and was thus excluded from the model. In the York basin the model *Gmax* only explain 17% of the variation.

The two variables related to pre-flood rainfall, *Rain_sum* and *Rain_int*, are good predictors of *Qmax* only in four basins: Bécancour, Batiscan, Matawin, and Ouelle. Combined with *Gmax*, soil moisture and *Rain_sum* it explained 70% of *Qmax* in the Bécancour basin. In Matawin it is combined with soil moisture and explains 40% of the variation, while in the Ouelle basin it is combined with melt intensity to explain 30% of the variation. Soil moisture was thus found to be a significant predictor in only two basins. In Bras du Nord, *Qmax* could not be explained by any of the predictors considered.

Interannual variations in peakflow timing (DOY) *Qmax_T* are comparatively well explained by a different combination of factors between basins, with adjusted R^2 varying between 0.4 and 0.7. (Table 7). Rain intensity explains most of the variation in the four basins Acadie, Nicolet, Bécancour and Ouelle and rainfall sum in the Etchemin basin. In the three basins York, Bras du Nord and Matawin, most of this variation is explained by pre-flood snowmelt *Melt_sum*. For Famine and Beaurivage maximum SWE *Gmax* is the main predictor. Soil moisture is the main predictor only for the Godbout basin.

Uncertainties of simulated predictors

Overall, the linear models explain more than 36% of the variation of *Qmax* in only five basins and for the seven other basins the antecedent variables explain less than 30% of the variation. Additionally, for Bras du Nord *Qmax* is not explained by any of the variables considered while in Bécancour it is explained only by soil moisture, which appears little logical for a nival basin. The question here is why do these weak correlations occur? Candidate explanations could be the existence of other, unaccounted factors such as large-scale climatic indices and pre-freezing soil moisture or bad simulations by the model.

Soil moisture and SWE were simulated by a conceptual model. Hence, the capacity of these simulated factors to explain the characteristics of observed streamflow is strongly dependent on the quality of the model simulation. Additionally, all the preconditionning factors were calculated considering the transfer time of the basin (x4) which is a calibrated routing parameter, which can result in events occurring shortly prior the flow peaks not being taken into account if this parameter is over estimated, especially given that rainfall events falling on snow or frozen ground can cause rapid runoff. The calibration and validation results obtained by Nemri and Kinnard (2019) (Table 4) show an overall good performance for all basins in the simulation of streamflow and SWE. Nevertheless, the Nash criterion used for calibration and validation is a global performance criterion calculated over the whole period and reflects the overall ability of the model to simulate the basin water balance, and as such does not guarantee accurate simulations for all years. For some basins, the spring peakflow is not well simulated in several years even if the model shows a good global performance during calibration/validation. The comparison between the yearly observed and simulated maximum streamflow *Qmax* (Fig. 7) shows that the worst simulation occur in the two basins Bécancour and Bras du Nord (B3 and B9 in Fig. 7). This under-estimation or overestimation of simulated spring flow can be related to a bad simulation of antecedent hydrological conditions, used here as flood drivers, to simulate these peaks. This can explain the weak correlation found between *Qmax* and the antecedent factors obtained for these two basins (cf. Fig. 5 and Table 6). Additionally, after inspecting the hydrograph over several years we can notice that for some basins the hydrological response to an important rain event can be more rapid than the calibrated time of transfer (x4). The impact of this parameter on the peakflow magnitude and timing explanation by antecedent factors was thus assessed by reducing the transfer time to zero, one or two days depending on the basin in order to check the improvement of the regression models resulting from this modification. Also, in some basins peakflow can be seen to be generated by an important event over a one or two day period, while the factors used here (*Rain_int*, *Melt_int*) were averaged over the whole pre-flood period, i.e. between the onset date and the hydrograph peak, and which can last more than seven days in some years. Thus, two additional factors were added, namely the rainfall and snowmelt maximum intensity over the pre-flood period to reflect this phenomenon and reduce the uncertainty related to using mean intensities only. After changing the transfer time and taking into account these two factors, the linear models of *Qmax* interannual variations improved for many basins as summarized in Table 8. The regression models explain more than 47% of the variation in all basins except the Batiscan and Beaurivage basins where the models still explain only 20% of the variation. For Bras du Nord, although the Nash_SWE in calibration was 65% (Table 4), after yearly verification we noticed that in 11 years out of 50, the SWE was not well simulated by the Cemaneige model. After changing the number of routing days (x4) to zero, which was initially calibrated to two days, the R^2 increased from zero to 40% with variations of *Qmax* being explained by rain intensity and melt intensity (Table 8). For the Beaurivage basin, the initial linear model explained only 11% of the variation using melt intensity. The SWE is well simulated globally in calibration and validation with Nash_SWE equal to 72% and 79% respectively. Even after changing the transfer time from two days to one or zero day the model still only explains 20% of the variation, with melt intensity as sole predictor. For the Matawin basin the SWE simulation is the worst in calibration (31%) compared to the other basins. Changing the transfer time from 4 to 2 days improved the linear regression model (R^2 from 37 to 50%) with *Qmax* being explained by rain intensity, melt intensity, melt sum and soil moisture. The initial model only explained 15% of *Qmax* in the Nicolet basin with *Gmax* as sole predictor. After changing the transfer time to one day the linear model explains 44% of the variation of *Qmax* by rain intensity, maximum melt intensity, and soil moisture. The simulation of SWE in this basin is rather good in calibration (50%) and validation (70%). In the York basin the SWE is well simulated globally in calibration (57%) but the simulation is poor in several years. Changing x4 from 2 to zero days improved the regression model from 20% to 52% with *Qmax* variations explained by rain and melt intensity and soil moisture. In the Famine basin the SWE is well simulated in calibration (84%) and validation (76%) and the regression R^2 increases from 36% to 44% with *Qmax* explained by melt intensity, rain sum and *Gmax* after changing the transfer time from 2 to 1 day. For Godbout basin the simulation of SWE in calibration is rather good (50%), the modification of x4 (2 to zero day) improved the regression from 35% to 54% with *Qmax* explained by rain and snow melt intensity and rain sum. For the four basins Batiscan, Etchemin, Bécancour and Acadie changing the transfer time to 0-2 days did not improve the models. Overall, the sensitivity of *Qmax* prediction by antecedent factors to the chosen transit time highlight the importance of snowmelt and rainfall events in the two days before the peakflows, and the difficult in deriving precise forecasts on longer lead times.

Extremes events as simulated by conceptual model

To better understand the results of the linear regression analysis we tried to disentangle the mechanisms leading to the historical largest peakflow events and the main hydrometeorological factors behind these extreme events as simulated by the model. For the sake of brevity we only consider the four years with the largest spring flow peaks for the twelve basins as summarized in Fig. 8. In the southernmost Acadie basin, the mean of *Qmax* over the period 1980-2015 is 70 m^3/s. For the four years with the largest *Qmax* (123-219 m^3/s) (Fig. 8B1), peak SWE was above the period average (*Gmax* = 109 mm) with no rainfall events recorded except in 1998 when a rainfall event was recorded during snowmelt. Incidentally, the highest streamflow recorded in this basin was in 1998 and was the combined result of an above-normal snowpack (*Gmax* = 194 mm) and an important rainfall quantity. Still, the linear regression results showed that 60% of the variations in *Qmax* is controlled only by melt intensity, which was the case for the three other extreme years. In Nicolet, located in the St. Laurent southwest hydrologic region characterized by a maritime and continental climate, and in the Appalachian Mountains physiographic region, mean *Qmax* was 390 m^3/s over the period 1967-2015. The four years with highest peakflows (560-762 m^3/s) were not generated by exceptional snowpack as *Gmax* was near its historical average (211 mm) (Fig. 8B2). No exceptional rainfall events were recorded during the pre-flood period in 1982 (*Qmax* = 663 m^3/s) and 1998 (*Qmax* = 560 m^3/s). Therefore, snowmelt rate, ice-jams or frozen saturated soils could be the factors behind these exceptional events. The exceptional peakflows of 1976 (614 m^3/s) and 1989 (762 m^3/s) were accentuated by a small one-day rainfall event during melting (30 mm). The regression analysis confirms these observations where 44% of *Qmax* variations were explained mainly by pre-flood maximum melt intensity and secondly by rainfall intensity. Mean *Qmax* was 460 m^3/s over the period 2000-2015 in the Bécancour basin, where important rainfall events were recorded during snowmelt in the four years with highest peakflow (514-814 m^3/s) (Fig. 8B3). The maximum simulated SWE in these years were very close to the period average (230 mm). The extreme flood of 2014 (814 m^3/s) recorded in this basin was accentuated by six rainy days before the peak while no exceptional maximum SWE was recorded for this year. In 2011, the peak (540 m^3/s) was generated mainly by a few long rainy days just at the end of the melting period following a previous peak generated by snowmelt (420 mm). Therefore, for this basin extreme events are not generated by an exceptional snowpack but rather by a combination of rainy days and melting. The regression analysis showed that 74% of *Qmax* variations are explained by rain sum, maximum SWE and soil moisture. For the Famine basin mean *Qmax* was 163 m^3/s over the period 1965-2015 and in the four years with extreme spring flow (265-299 mm), important rainfall events are recorded (Fig. 8B4). In 2008 an important snowpack (peak SWE = 400 mm) accentuated by rain events were at the origin of important streamflow, but the largest peakflow (286 m^3/s) occurred after peak snowmelt and was triggered by a large rainfall event. A similar pattern occurred in the next year 2009, although with a snowpack thinner than average. The linear regression models confirm that 44% of the variations in *Qmax* are explained by mean melt intensity, rain sum and maximum SWE (*Gmax*). In the Batiscan basin, mean *Qmax* was 560 m^3/s for the period 1968-2015 and the four highest maximum peak flows varied between 761-837 m^3/s (Fig. 8 B5). An thick snowpack was recorded in 2008 (*Qmax* = 820 m^3/s; *Gmax* = 411 mm) and 1997 (*Qmax* = 773 m^3/s; *Gmax* = 360 mm) unlike the two years 1983 and 1970 when the maximum SWE was close to the period average (280 mm) but important rainfall events occurred during melting, which is confirmed by the linear models explaining only 28% of *Qmax* variations by rain intensity and melt sum. Mean *Qmax* was 180 m^3/s and mean peak SWE was 271 mm in the Beaurivage basin for the period 1961-2015, while the highest maximum peakflows varied between 270 and 325 m^3/s (Fig. 8B6). In the year 2014 with highest *Qmax* (325 m^3/s) important rain events are recorded with normal snowpack conditions. In the other three years the maximum SWE is close to average with little to no rainfall events, meaning that these peaks were generated by rapid melting, perhaps over saturated soil. Also, after checking the shape of the hydrograph in this basin we found that at least in 60% of years the hydrograph had a multi-peak shape which explains the poor correlation between the highest flow and the quantity of snow accumulated. This multi-peak shape can affect the length of the pre-flood period and subsequently the calculation of and influence of preconditioning factors. Also, 60% of this basin is forested while the rest is agriculture, and snowmelt in forests is typically slower than in open fields which is the reason behind this peak multiplicity. This is confirmed by the linear model that explained only 20% of the variation by melt intensity. In the Matawin basin the four highest maximum spring flows vary between 210 and 240 m^3/s (Fig. 8B7). No exceptional snowpacks were recorded but a combination of important rainfall events occurred during melting and are at the origin of the important peakflows in 1983 and 1998. In 2008 an important snowpack was recorded (250 mm) compared to the annual mean period average (159 mm), with no rainfall recorded, while in 2002 the maximum SWE was close to average (159 mm) also with no rainfall events, so runoff generation must have been induced by rapid melt and/or saturated soil. The linear model explains 50% of the variations in *Qmax* by the melt intensity, mean rain intensity, *Gmax* and soil moisture. In the four years with highest maximum spring flow (330-369 m^3/s) in the Etchemin basin (Fig. 8B8) an thick snowpack was simulated by the model along with important recorded rain events, so runoff was mainly generated in these years by the combination of these rainfall events during melting. Conversely, the linear model explains 40% of the variations in *Qmax* only by melt intensity and maximum SWE. In Bras du Nord the highest four maximum spring flows varied between 235 and 277 m^3/s (Fig. 8B9). In 1994, no exceptional snowpack was recorded for that year, with maximum SWE being close to average (350 mm), and the extreme spring flow (235 m^3/s) was generated after snowmelt by a large rainfall quantity. For the three other years (1968, 1997, 1989) peakflows seem to have been generated by a combination of snowmelt and significant rainfall events with snowpaks close to average. On the other hand, the peak snowpack recorded in two years 2008 (516 mm) and 1972 (531 mm) (not shown in the figure) are above average but the observed peakflow was so close to the average streamflow. The linear regression model showed for this basin that 40% of the variations in *Qmax* are controlled by rain and melt intensity, which means that in the large forested basins a lot of the slow snowmelt is infiltrated during snowmelt but any large intensity event (snowmelt and or rainfall) results in rapid runoff. In the Ouelle basin, important rainfall events were recorded during melting for the four extreme years and only in 2008 was the accumulated snowpack important (*Gmax* = 405 mm) and above the period average (*Gmax* = 281 mm) (Fig. 8B10). For this basin *Qmax* is controlled mainly by maximum melt and rain intensity which explain 53% of the inter-annual variation. For the York basin (Fig. 8B11) important rainfall events are recorded during the four years with extreme *Qmax* (200-280 m^3/s) combined with important snowpack above the period average (*Gmax* = 376 mm) in 1981 (*Gmax* = 479 mm) and close to the average for the other three years. After the change of X4 calibrated for this basin the improvement of the stepwise model was by an interaction term (-0.308) between melt intensity *Melt_int* and soil moisture model which means that more rapid snowmelt leads to decreased peakflow which is not logical. The VIF coefficient (not shown here) is 8 so acceptable it is not a problem of multicollinearity between these two factors but a limitation of stepwise method that will be discussed later in this paper. In the Godbout basin, mean *Qmax* was 310 m^3/s over the period 1975-2015. For the four years with most extreme peakflows (456-856 m^3/s), important rainfall events were recorded during melting, with normal snowpack simulated by the model (Fig. 8B12). In fact, in several other years where an important peak SWE (*Gmax*) was simulated but the resulting peakflow remained close to average conditions. For example, in the extreme event of 1979 (865 m^3/s) the maximum SWE was less than the period average and runoff was generated by an extreme rainfall event during snowmelt. Important rainfall events are also recorded during melting in the other extreme years. The linear regression results for this northernmost basin showed that 60% of *Qmax* variations are explained by rain intensity, melt sum and rain sum.

Hence for all these snow-dominated basins the extreme events recorded were not only generated by a large snowpack but by a combination of rainfall and snowmelt events. For the majority of forested basins, few of the extreme peakflow events were associated with exceptional snowpacks. A pattern may be emerging, that snowmelt is generally slower in forested basins, which makes them less sensitive to peak SWE, but more sensitive to the intensities of melt and rainfall events. Conversely in the southernmost and more agriculture Acadie basin, extreme events are generated by exceptional snowpacks with rapid snowmelt intensity.

Discussion and conclusion

Understanding the inter-annual variability of the observed characteristics (magnitude and timing) of the spring freshet in response to the contribution of antecedent hydrological conditions (peak SWE, melt rate, rainfall, soil moisture) in the generation of runoff was always challenged by the lack of observed data, especially snow cover and soil moisture. Lumped hydrological models coupled with a temperature-index snowmelt model give accurate simulations of snow cover and discharge overall, but spring peakflow can sometimes be under or over-estimated in some years as found in this study. The improvement of results after changing the calibrated transfer time shows that the results of the multivariate regression models are strongly dependent on the performance of the model to correctly simulate all antecedent variables for all the years. The snowpack melt rate, which is controlled by the energy balance, can be rapid or gradual in relation to the spring air warming rate and the presence of vegetation.

Melting is more gradual in forests and faster in areas with cleared forest and agriculture, which can increase the magnitude of flow peaks (Ellis et al., 2011). However, the spatial distribution of the snow cover and the spatial variability of snowmelt is not taken into account in the simple temperature-index snowmelt model, other than that induced by elevation. Moreover, the quantity of rainfall events during melting can generate more rapid runoff depending on the antecedent retention capacity of the snowpack (Ellis et al., 2011; Mccabe et al., 2007; Pomeroy et al., 2016; Sui et al., 2001) and the advected energy from this rainfall is also not considered in the simple model. In fact, liquid precipitation that occur in spring on the snowpack can be stored by the snowpack if it is initially dry and released later. Therefore, several uncertainties can arise from using simulated instead of measured snowpack conditions, especially since we found that SWE can be under-or overestimated in some years even if the model simulates SWE adequately on average.

Results found in this study using measured and simulated antecedent factors can improve our understanding of flow characteristics interannual variations. The mean melt intensity (*Melt_int*) calculated over the period from the flood onset date to the peakflow date is a good predictor of the peakflow magnitude (*Qmax*) in seven basins (Acadie, Famine, Beaurivage, Etchemin, Matawin, Bras du Nord and York) and is the most skillful predictor for four of these basins (Acadie, Famine, Beaurivage, Etchemin). The maximum melt intensity (*Meltint_max*) is a good predictor only in the Nicolet and Ouelle basins. So, overall, snowmelt intensity appears to be the dominant control on peakflow magnitude for 9 of the 12 basins. Also, the quantity of melt in the pre-flood period (*Melt_sum*) is the best predictor in Matawin and Batiscan and a significant contributor in the Godbout basin. The accumulated peak SWE simulated at the beginning of spring (*Gmax*) reflects the winter conditions of the year and was retained as a significant predictor of *Qmax* only in four basins (Nicolet, Bécancour, Famine and Etchemin) so years with higher snowpack result in higher peak spring streamflow. Still, *Gmax* by itself could explain 10 to 28% of the variability in *Qmax* in 8 out of 12 basins as shown by the bivariate correlation analysis (Fig. 5). This shows that the memory of the snowpack is not sufficient to accurately forecast springtime flood magnitude in southern Quebec. Overall, for the eight basins located in more southerly latitudes (basin ID 1-8) peakflow magnitude variability is primarily controlled by snowmelt intensity and quantity, and only in four basins do factors related to rainfall contribute to explain peakflow variations.

Mean rainfall intensity (*Rain_int*) during the pre-flood period is the most skilful predictor in three basins (Bras du Nord, York and Godbout) and a significant predictor in the two basins Matawin and Batiscan. The maximum rainfall intensity (*Rainint_max*) was the most skilful factor in the Ouelle basin only. The pre-flood rainfall quantity (*Rainsum*) is contributing to peakflow variations only in four basins (Ouelle, Godbout, Famine and Bécancour). So, for the four northernmost basins (Bras du Nord, Ouelle, York and Godbout), variations in peakflow are mainly controlled by rain events (intensity and sum) during the melting period. Soil moisture was considered to be a key factor in controlling runoff in snow-dominated basin in several studies (e.g. Wever et al., 2017). In this study, no coherent correlation was found between the degree of soil saturation and peakflow variations. Even within the multivariate regression analysis this factor was found to be a significant predictor of peakflow magnitude and timing only for three basins, and a counterintuitive negative effect was found for two of these basins. The lumped GR4J model does not consider soil freezing processes. Therefore, further research is needed in Quebec basins using a physically-based model that explicitly represents soil freezing and fall moisture 'soil memory' in order to better simulate pre-melt soil moisture and its effect on snowmelt and rainfall runoff. Soil freezing is often assumed to play an important role on infiltration, but deep snowpacks can also inhibit soil freezing and cancel its impact on infiltration (Aygun et al., submitted).

Overall, the ranking of preconditioning factors based on their frequency of appearance as significant factors in the linear models of *Qmax* across the twelve basins is as follow: (i) melt intensity (mean and max), (ii) rain intensity (mean and max), (iii) the sum of melt, (iv) sum of rain, (v) peak SWE (*Gmax*) and (vi) soil moisture. One note of caution must be mentioned, that the stepwise approach finds the best combination of factors explaining the most variations in *Qmax,* and as such can remove predictors that are still important on their own, but that are redundant (collinear) in a multivariate context. Still, melt intensity also appears as the most important univariate predictor of *Gmax* as shown by the correlation analysis (Fig. 6), but peakSWE (*Gmax*), which is the second best univariate predictor of *Qmax* (Fig. 6) was often excluded from the multivariate models. A thicker snowpack is more likely to survive later into the spring season and be subjected to faster melt rates (e.g. Musselman et al., 2017) , which could explain the redundant predictive power of these two variables in multivariate models.

The peakflow timing is controlled in most basins by the rainfall sum and intensity factors. These results are not in agreement with these found by Curry et al. (2017) in western Canada for the Fraser River basin in between the Coast Mountains and the Continental Divide, where the generation of spring runoff is controlled mainly by the maximum accumulated SWE and secondly by the melt rate. On the other hand Coles et al. (2016) found that the processes responsible for the generation of runoff in the Canadian prairies hillslopes were mainly and in order of importance the total snowfall, snow cover amount, fall soil surface water content (0-15 cm) and melt rate. The more humid climate of southern Quebec compared to the Canadian Prairies, and the lower elevation compared to the mountainous basins of western Canada, could explain the fact that interannual variations in accumulated SWE are generally less important than the melt rate and the quantity and intensity of rainfall events during snowmelt. Interannual changes in snowmelt volumes are either the prime driver, or equally as important than rainfall, in controlling flood volume variability as shown in Table 5. However regression analysis showed that snowmelt variables appear to be more important drivers of peakflow interannual variability for the more agricultural southern basins, even in the southernmost Acadie basin where snowmelt contributes less water than rainfall to flood volumes. Conversely in the more northerly, forested basins flood volumes are primarily controlled by snowmelt volumes in these nival basins whereas rainfall stands out as more important in controlling interannual variations in peakflow.

Initial conditions (snow stored in the basin, soil moisture) and their forecasting skill are very important for the seasonal prediction of streamflow (Foster et al., 2018; Koster et al., 2010; Li et al., 2009; Mahanama et al., 2012) but these variables are not well measured in most basins. Turcotte et al. (2010) discussed the difficulties envisaged by the prediction systems developed for Quebec basins due to errors in the snow observation methods. Therefore, using satellite products of snow cover in conjunction with physically-based models might be a good way to improve our understanding of the spring freshet generation mechanisms and the independent role of snow cover, rain on snow events and the soil moisture status in future studies Quebec.

List of tables

Table 1. Characteristics of the twelve basins selected in this study ranked according to latitude, from South to North.

ID	Basin	Lat. (°)	Lon. (°)	Area (km²)	Water %	Forest %	Agri-culture %	Alt. med. (m)	Low-lands %	Can. Shield %	Appala-chian %	Flow data
1	Acadie	45.39	-73.37	367	0	25.7	72.1	31	100	0	0	1979/2017
2	Nicolet	46.06	-72.31	1550	0	74.8	25.2	203	0	0	100	1966/2017
3	Bécancour	46.31	-71.45	2163	0	74.8	25.2	273	0	0	100	1999/2017
4	Famine	46.1	-70.30	696	0.3	87.4	12.3	377	0	0	100	1964/2017
5	Batiscan	46.59	-72.40	4504	0.7	92	6.7	385	0	100	0	1967/2017
6	Beaurivage	46.66	-71.29	708	0	61.3	38.7	152	0	0	100	1925/2017
7	Matawin	46.68	-73.92	1387	3.1	96.9	0	481	0	100	0	1931/2017
8	Etchemin	46.69	-71.07	1152	0	74.5	25.5	382	0	0	100	1980/2017
9	Bras du Nord	47.00	-71.80	646	0	100	0	597	0	100	0	1965/2017
10	Ouelle	47.38	-69.95	796	0.5	97.4	2.1	348	0	0	100	1982/2017
11	York	48.81	-64.92	647	0	100	0	482	0	0	100	1980/2017
12	Godbout	49.33	-67.65	1577	0.5	99.5	0	368	0	100	0	1974/2017

Table 2. Selected antecedent variables.

Factors	Unit	Description
Gmax	mm	Maximum of SWE simulated by the model on the first day of spring (1^{st} Mars)
Rain_int	mm/d	Mean of rainfall intensity calculated over the pre-flood period
Rain_sum	mm	Rainfall sum during the pre-flood period
Melt_int	mm/d	Mean of snowmelt intensity calculated over the pre-flood period
Melt_sum	mm	Sum of snow melt
Smean	()	Mean of soil reservoir saturation degree

Table 3. Interannual variability of spring maximum flow and its date of occurrence.

ID	Basin	Nb of years	Min Qmax (m^3/s)	Max Qmax (m^3/s)	Mean Qmax (m^3/s)	Std Qmax (m^3/s)	Occurrence month (nb years)			
							Mar.	Apr.	May	June
1	Acadie	36	12	219	71	42	15	15	4	2
2	Nicolet	49	161	762	390	130	15	31	2	1
3	Bécancour	16	235	814	446	134	2	12	2	0
4	Famine	51	13	299	163	57	7	40	3	1
5	Batiscan	48	295	837	563	141	0	33	13	2
6	Beaurivage	55	50	325	180	52	9	41	4	1
7	Matawin	43	60	240	153	41	2	28	13	0
8	Etchemin	35	158	369	253	62	6	27	2	0
9	Bras du Nord	51	63	277	156	48	0	20	28	2
10	Ouelle	33	87	427	218	82	2	22	9	0
11	York	35	50	280	141	47	0	3	32	0
12	Godbout	41	108	856	310	132	0	4	37	0

Table 4. Results of GR4J-CEMANEIGE model using AMALGAM multi-objective algorithm (Nemri and Kinnard, 2019) for the six parameters x1: capacity of production store (mm); x2: water exchange coefficient (mm); x3: capacity of routing store (mm); x4: UH time base (days); x5: Cemaneige snow pack thermal state; x6: Cemaneige degree-day melt coefficient.

Basin	x1 (mm)	x2 (mm)	x3 (mm)	x4 (days)	x5 ()	x6 (mm °C^{-1})	Nash_flow calib	Nash_swe calib
Acadie	200	-0.95	42	2	0.01	6.1	63	33
Nicolet	217	0.22	36	2	0.01	5.9	76	50
Bécancour	216	-0.6	87	2	0.29	5.5	76	84
Famine	25	0.27	97	2	0.3	3.2	83	84
Batiscan	436	0.5	134	3	0.03	4.4	90	49
Beaurivage	44	-0.7	66	2	0.62	4.1	72	72
Matawin	117	-0.51	351	4	0.05	4.6	90	31
Etchemin	24	-0.33	238	2	0	7.2	80	56
Bras du Nord	346	-0.59	112	2	0	4.8	84	65
Ouelle	64	0.29	79	2	0.44	3.7	81	70
York	78	-0.55	115	2	0.39	2.9	85	57
Godbout	265	5.1	305	2	0.03	7.1	82	49

Table 5. Linear regression of response variable (runoff volume) against vertical inflows (snowmelt and rainfall) during the pre-flood period. Standardized regression coefficients (β) indicate the relative influence of melt and rain volumes to interannual variability in flood volume. The adjusted coefficient of determination (R^2) indicates the strength of the relationships.

ID	Basin	β1: Rainsum	β2: Meltsum	Adjusted R^2
1	Acadie	0.6	0.6	0.83
2	Nicolet	0.5	0.6	0.81
3	Bécancour	0.3	0.9	0.89
4	Famine	0.3	0.8	0.82
5	Batiscan	0.5	0.6	0.93
6	Beaurivage	0.3	0.8	0.67
7	Matawin	0.6	0.5	0.88
8	Echemin	0.2	0.7	0.72
9	Bras du Nord	0.5	0.6	0.92
10	Ouelle	0.4	0.7	0.85
11	York	0.3	0.8	0.88
12	Godbout	0.4	0.7	0.72

Table 6. Results of stepwise multivariate regression of spring flow magnitude against the six antecedent factors (predictors) for the twelve basins.

Basin	Standardized regression coefficients						Adjusted R^2	p value
	Rain_sum	Rain_int	Melt_sum	Melt_int	Gmax	Smean		
Acadie				0.75			0.56	0.000
Nicolet					0.41		0.15	0.003
Bécancour	0.42				0.51	-0.71	0.74	0.000
Famine			0.32	0.45			0.36	0.000
Batiscan		0.29	0.59				0.28	0.000
Beaurivage				0.35			0.11	0.013
Matawin	0.37	0.56				0.28	0.38	0.000
Etchemin				0.51	0.33		0.39	0.000
Bras du Nord								
Ouelle	0.37			0.56			0.30	0.007
York					0.46		0.17	0.005
Godbout				0.47			0.20	0.002

Table 7. Results of stepwise multivariate regression of occurrence date of Qmax_*T* (DOY) against the antecedent factors (predictors) for the twelve basins.

Basin	Standardized regression coefficients						Adjusted R^2	p value
	Rain_sum	Rain_int	Melt_sum	Melt_int	Gmax	Smean		
Acadie	0.31	0.5				-0.4	0.50	0.000
Nicolet	-0.38	-0.38					0.38	0.000
Bécancour		1.13	0.7				0.65	0.000
Famine		0.49			0.59	0.49	0.61	0.000
Batiscan	0.18			-0.36	-0.36		0.58	0.000
Beaurivage		-0.26		-0.26	0.26		0.56	0.000
Matawin	0.35		0.51				0.51	0.000
Etchemin	0.56				0.3		0.32	0.001
Bras du Nord	0.25		0.53				0.43	0.000
Ouelle		0.72			0.41		0.55	0.000
York			0.65			-0.32	0.37	0.000
Godbout	0.41	-0.64				0.42	0.67	0.000

Table 8. Results of stepwise multivariate regression of spring flow peak magnitude *Qmax* and the six antecedent factors (predictors) for the twelve basins after changing the transfer time (x4) and adding two antecedent factors of maximum intensity of rainfall and snowmelt. All Adjusted R^2 are significant with p-value < 0.0.1.

Basin	Standardized regression coefficients								Adjusted R^2
	Rain sum	Rain int	Melt sum	Melt int	Gmax	Smean	Rainint max	Meltint max	
Acadie				0.75					0.60
Nicolet					0.41			0.81	0.44
Bécancour	0.42				0.51	-0.71			0.74
Famine	0.39			0.433	0.31				0.44
Batiscan		0.29	0.59						0.28
Beaurivage				0.46					0.20
Matawin		0.33	0.51	0.28		0.24			0.50
Etchemin				0.51	0.33				0.40
Bras du Nord		0.59		0.41					0.41
Ouelle	0.52						1.16	0.44	0.53
York		0.49		-0.308		-0.308			0.52
Godbout	0.23	0.92	0.23						0.60

Table 9. Results of stepwise multivariate regression of spring flow peak timing *Qmax_T* (DOY) and the six antecedent factors (predictors) for the twelve basins after changing the transfer time (x4) and adding two antecedent factors of maximum intensity of rainfall and snowmelt.

Basin	Standardized regression coefficients								Adjusted R^2
	Rain sum	Rain int	Melt sum	Melt int	Gmax	Smean	Rainint max	Meltint max	
Acadie		0.61		-0.33					0.57
Nicolet	-0.50			-0.50					0.50
Bécancour		1.17	0.72						0.65
Famine		-0.14		-0.35	0.54	-0.14			0.55
Batiscan	-0.49			-0.49	0.51				0.53
Beaurivage	-0.54	0.55	0.44	-0.54					0.62
Matawin	0.52	-0.37	0.33						0.51
Etchemin	0.54								0.27
Bras du Nord	0.28		0.52						0.46
Ouelle		-0.34	-0.34						0.60
York	0.28		0.61			-0.34			0.48
Godbout	0.30	-0.65				0.42			0.64

List of figures

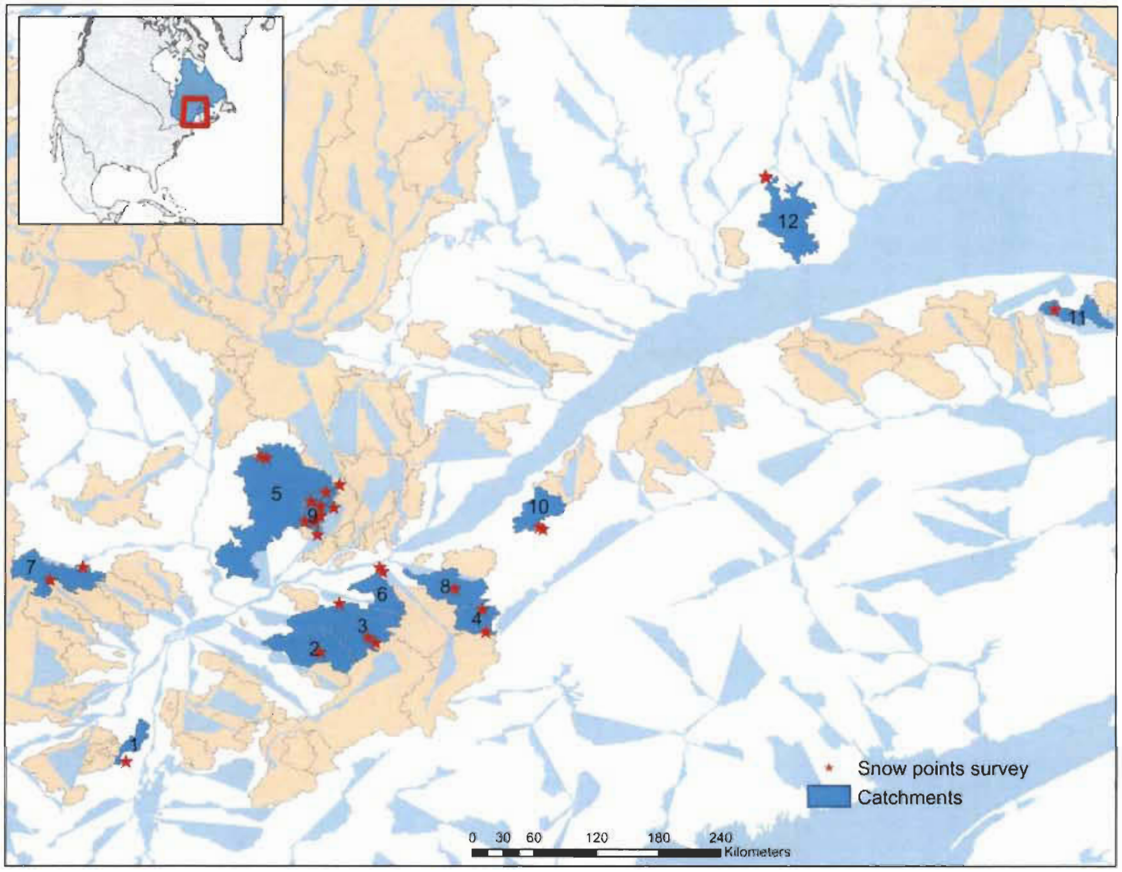

Fig. 1. Selected basins (blue) and snow survey measurement locations (red stars) in southern Quebec province. Basins ID : 1 Acadie, 2 Nicolet, 3 Bécancour, 4 Famine, 5 Batiscan, 6 Beaurivage, 7 Matawin, 8 Etchemin, 9 Bras du Nord, 10 Ouelle, 11 York, 12 Godbout. Basins IDs are ranked according to latitude, from South to North.

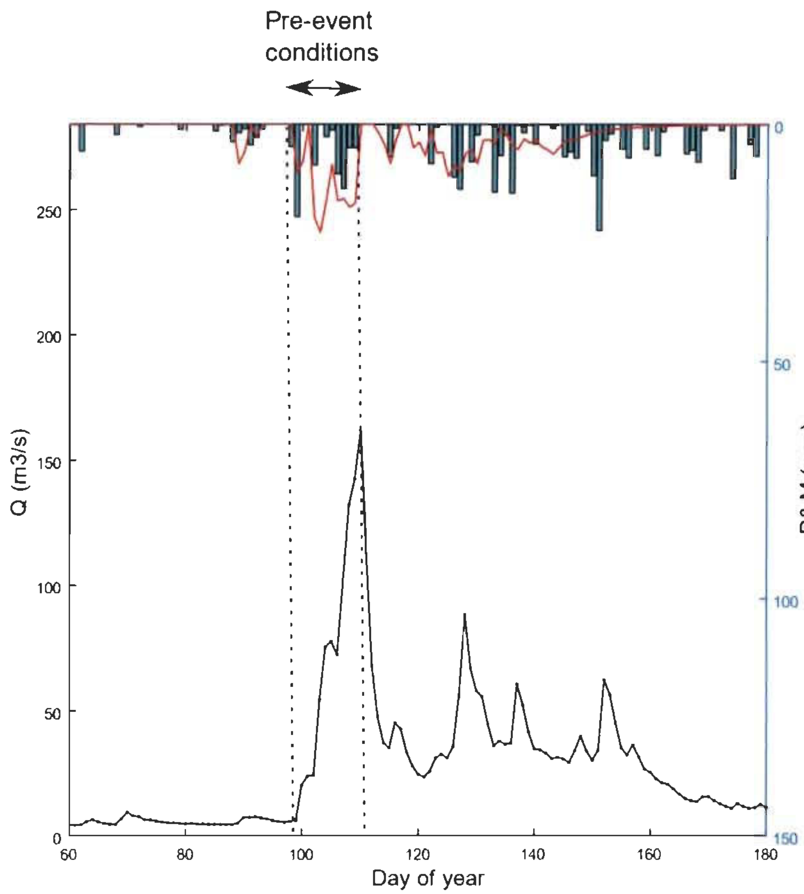

Fig. 2. Spring flood window from March to June and pre-event analysis period. The thick vertical stippled line indicates the automatically detected flood onset date and the thin vertical stippled line the peakflow date. The pre-flood analysis period extends from the onset date to x4 days before the peakflow date, where x4 is the transfer time (see text). Black curve: streamflow; blue bar: rainfall; red line: snowmelt.

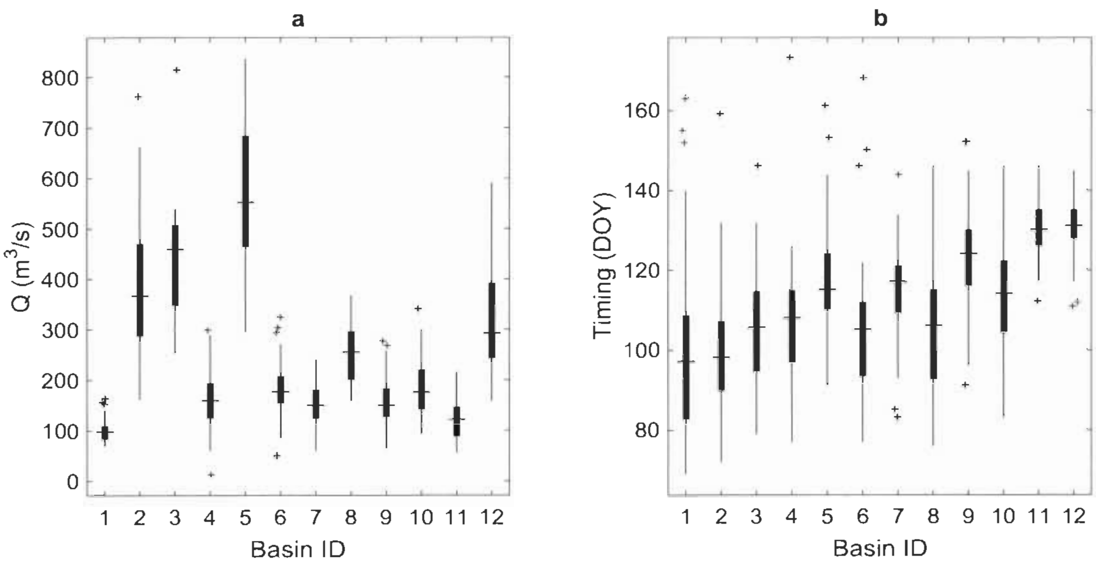

Fig. 3. Inter-annual variability of (a) spring *Qmax* (mm) and (b) spring *Qmax* timing (DOY) observed in the 12 basins.

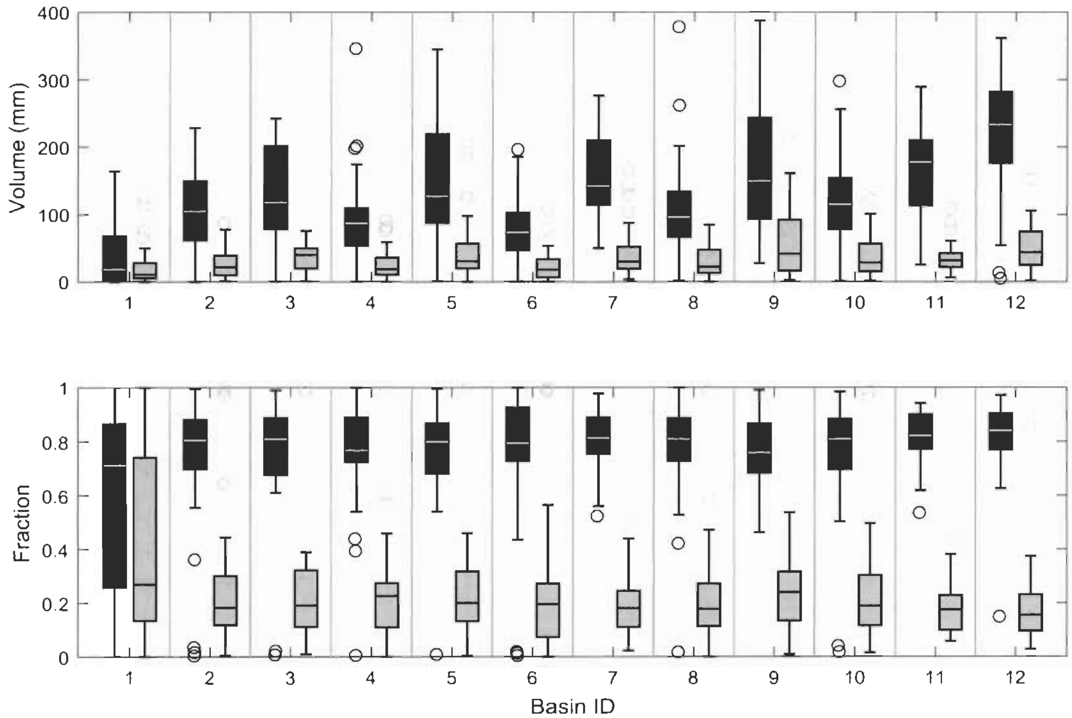

Fig. 4. Boxplots showing the distribution of (a) the snowmelt volume (black) and rainfall (grey) in the pre-flood period for each basin and (b) the relative contribution of these volumes to the total runoff volume during this period.

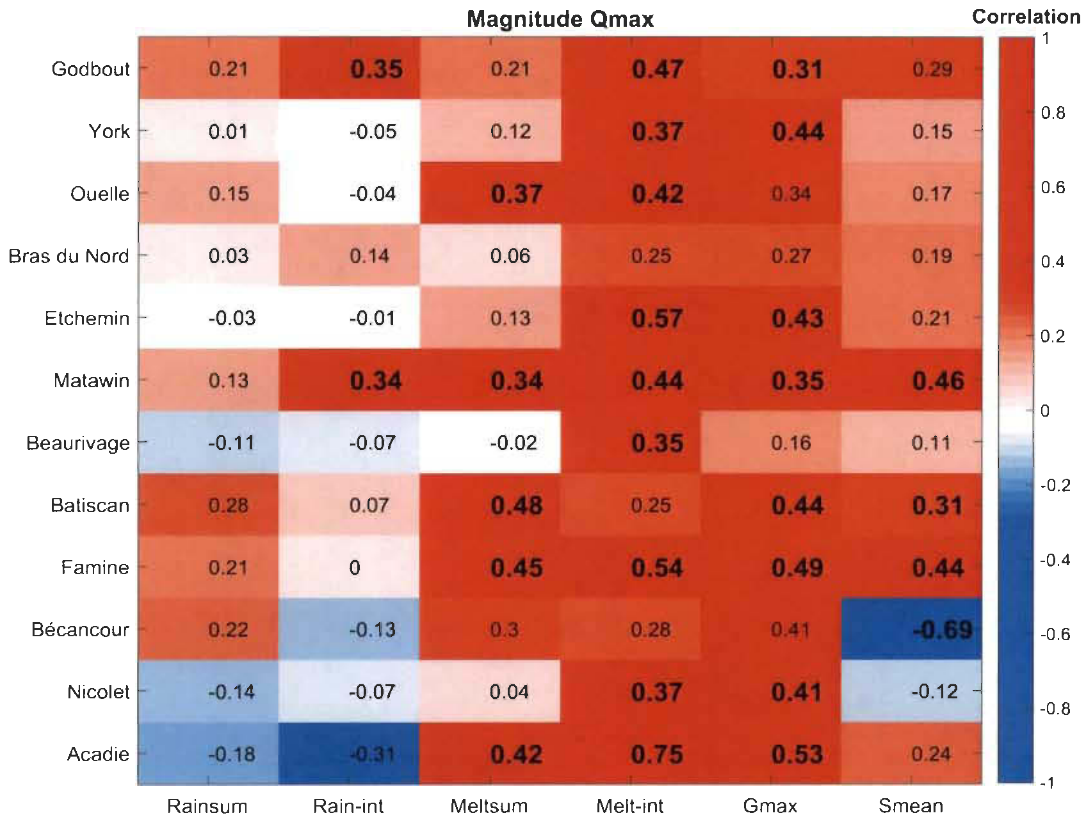

Fig. 5. Correlogram showing Pearson's linear correlation coefficient for all antecedent factors (columns) and spring flow peak magnitude (*Qmax*) for the twelve basins (rows). Significant correlation ($p < 0.05$) are highlighted in bold; blue colors indicate negative correlations and brown colors positive correlations.

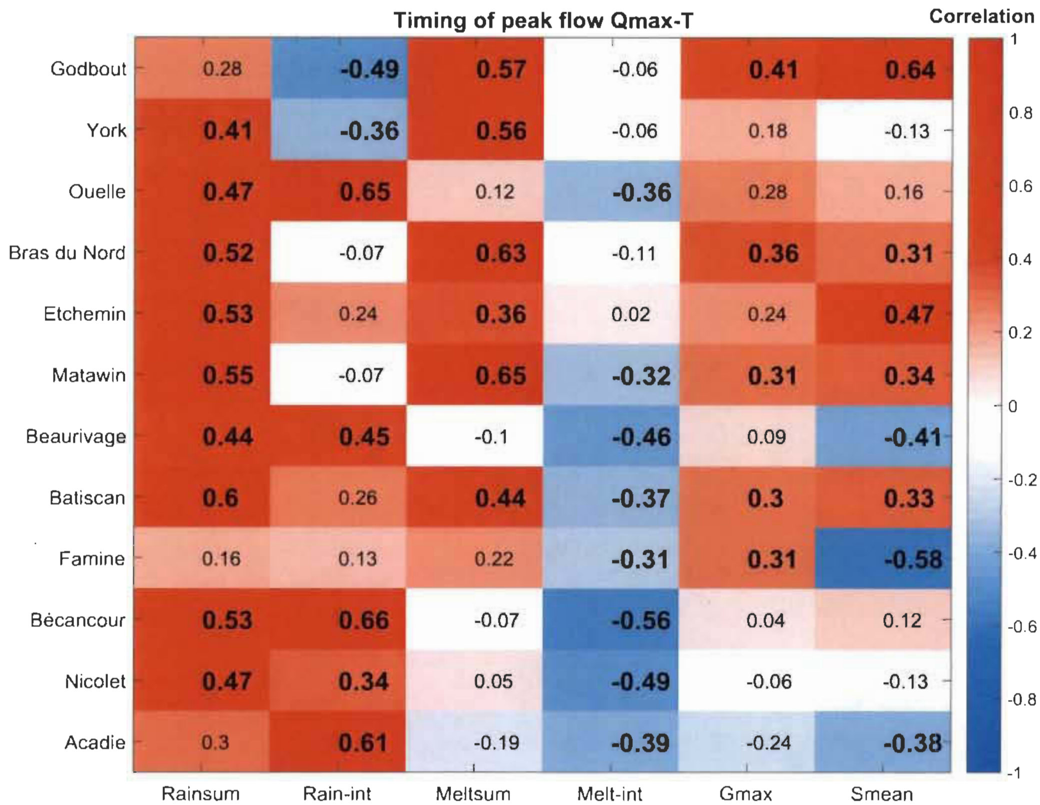

Fig. 6. Correlogram showing Pearson's linear correlation coefficient for all antecedent factors (columns) and day of occurrence (DOY) of peak spring streamflow *Qmax* for the twelve basins (rows). Significant correlation ($p < 0.05$) are highlighted in bold; blue colors indicate negative correlations and brown colors positive correlations.

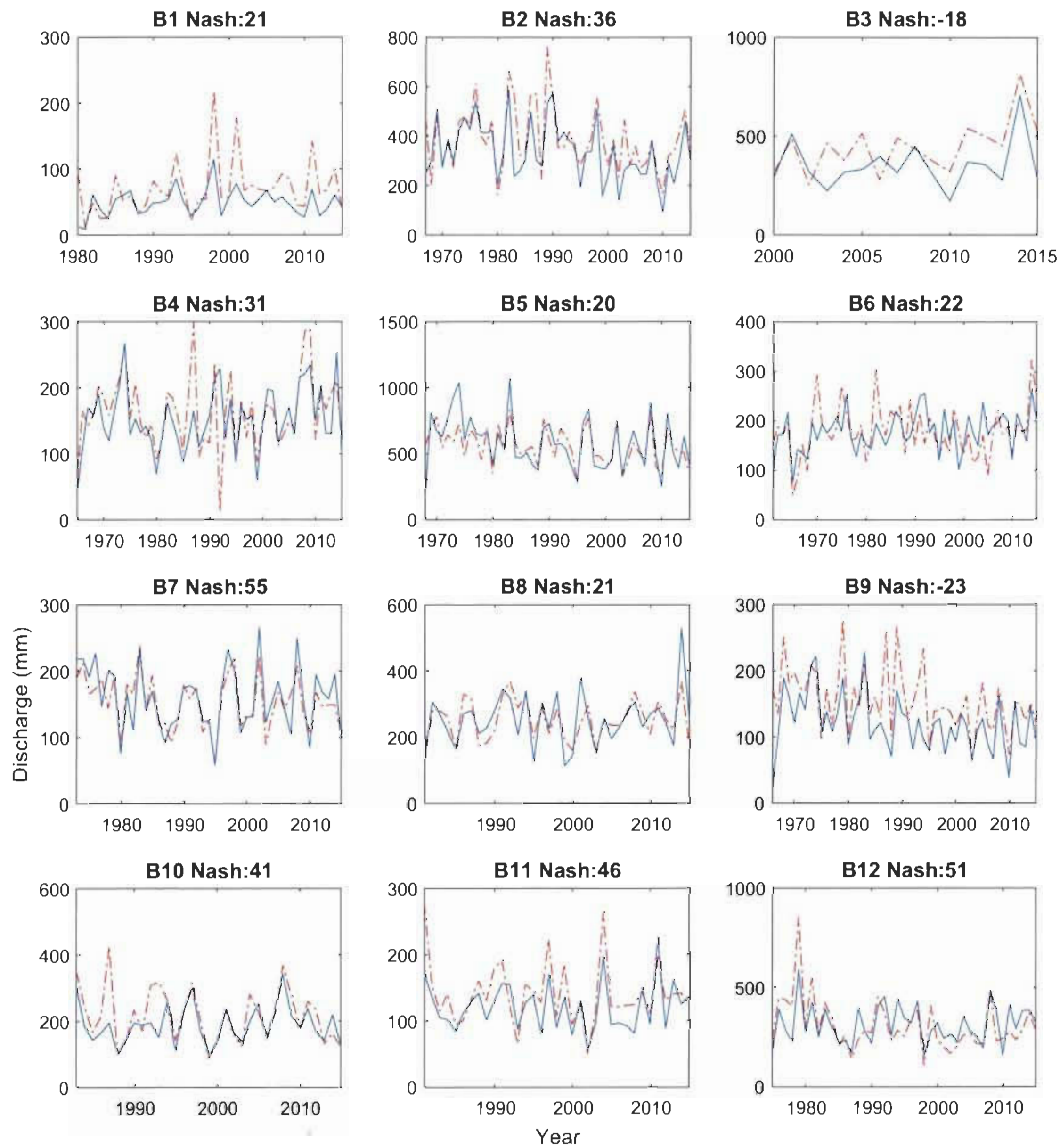

Fig. 7. Comparison of observed annual maximum spring streamflow *Qmax* (blue line) with that simulated by the GR4J model (red line) for the 12 basins and the Nash performance criteria calculated from the observed and simulated *Qmax*.

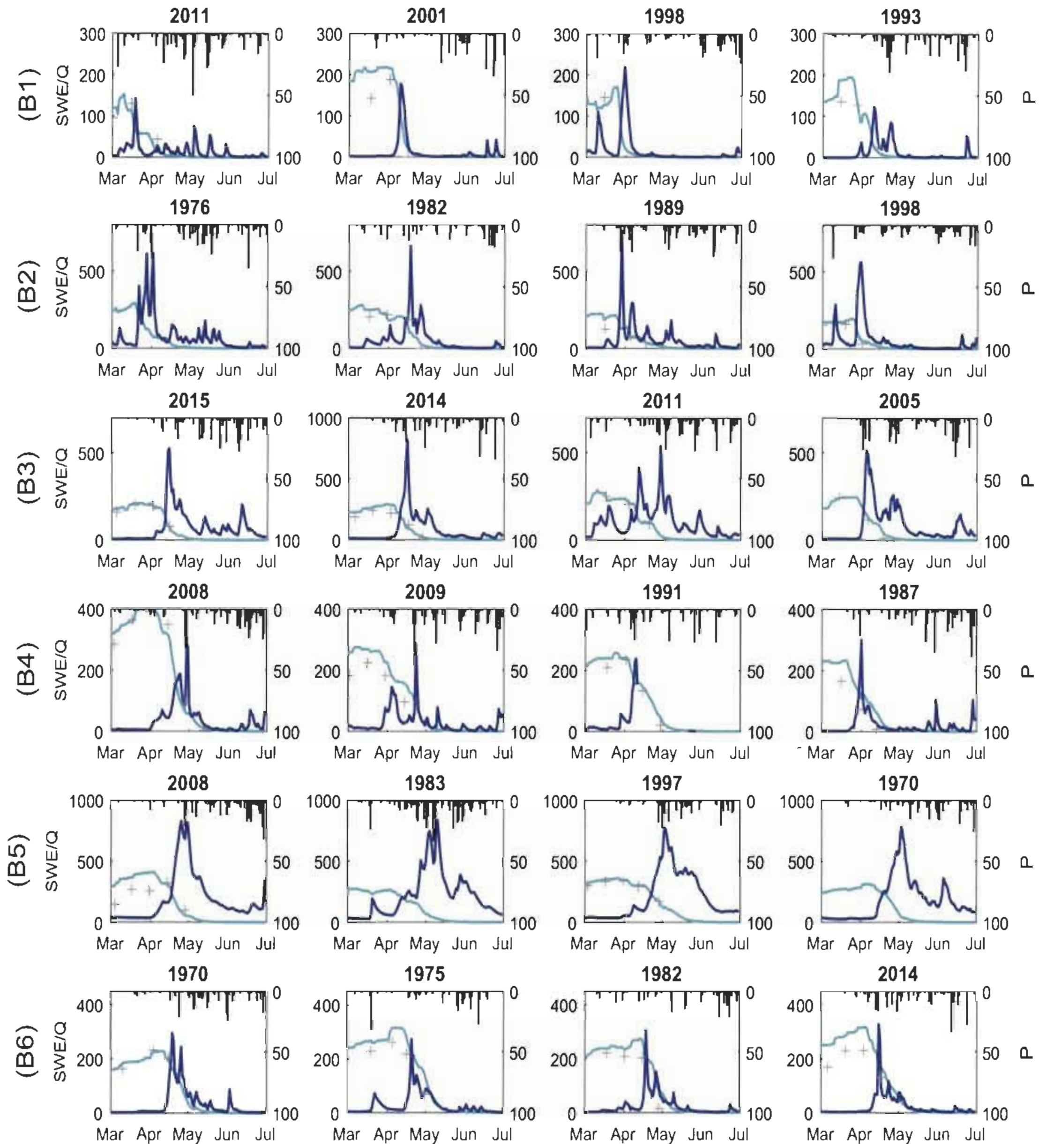

Fig. 8. Results of the four highest streamflow peaks for the twelve basins; B1) Acadie B2) Nicolet B3) Bécancour B4) Famine B5) Batiscan B6) Beaurivage. Observed streamflow Q (mm) shown in blue (left axis); simulated SWE (mm) shown in cyan (left axis); observed SWE (mm) shown as grey crosses (left axis); simulated liquid precipitation P (mm) shown as black bars (right axis).

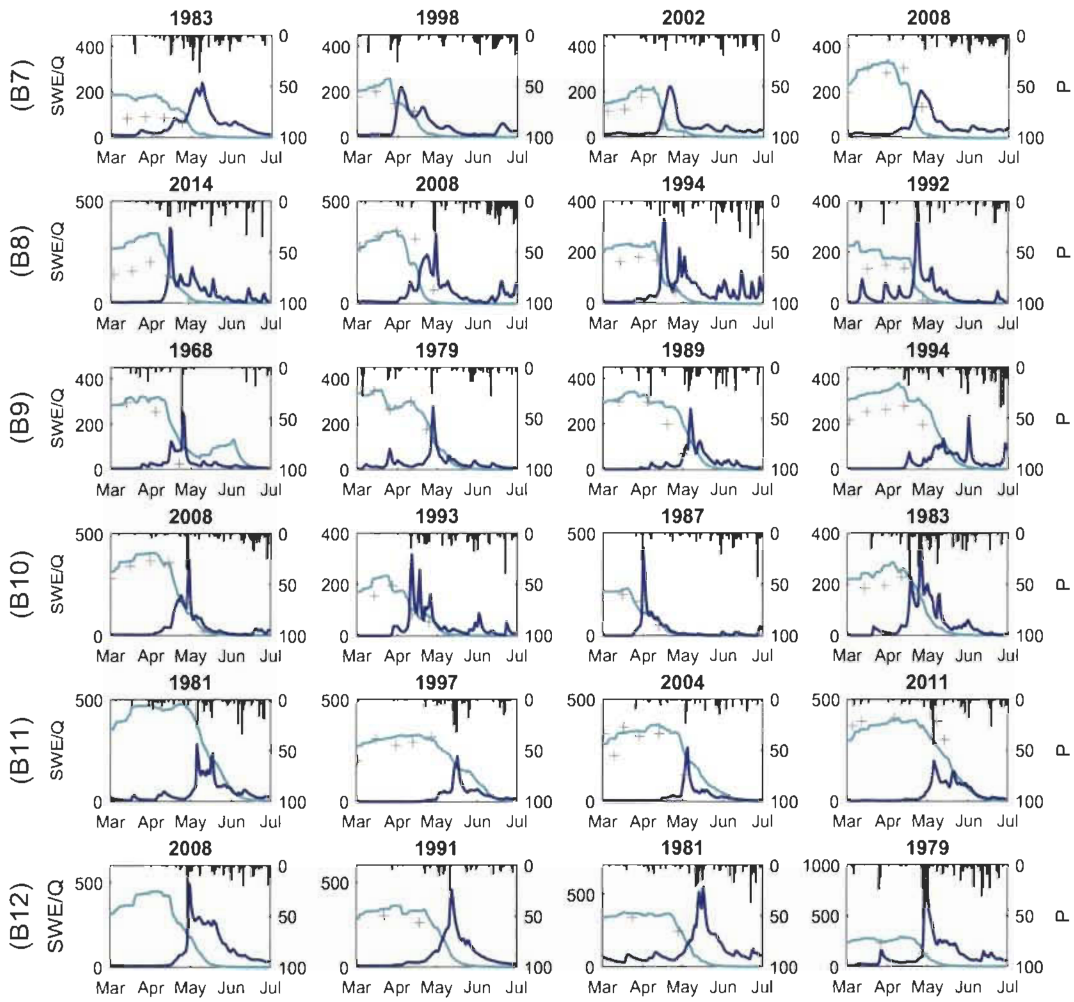

Fig. 8. (Continued) B7) Matawin, B8) Etchemin, B9) Bras du Nord, B10) Ouelle, B11) York, B12) Godbout.

References

Assani, A., Charron, S., Matteau, M., Mesfioui, M., & Quessy, J.-F. (2010). Temporal variability modes of floods for catchments in the St. Lawrence watershed (Quebec, Canada). *Journal of Hydrology, 385*, 292-299.

Assani, A., Charron, S., Matteau, M., Mesfioui, M., & Quessy, J.-F. (2010a). Temporal variability modes of floods for catchments in the St. Lawrence watershed (Quebec, Canada). *Journal of Hydrology, 385*, 292-299.

Assani, A., Landais, D., Mesfioui, M., & Matteau, M. (2010b). Relationship between the Atlantic Multidecadal Oscillation index and variability of mean annual flows for catchments in the St. Lawrence watershed (Quebec, Canada) during the past century. *Hydrology Research, 41*, 115-125.

Bergeron, J., Royer, A., Turcotte, R., & Roy, A. (2014). Snow cover estimation using blended MODIS and AMSR-E data for improved watershed-scale spring streamfow simulation in Quebec, Canada. *Hydrological processes, 28*, 4626-4639.

Bergeron, O. (2015). *Grilles climatiques quotidiennes du Programme de surveillance du climat du Québec, version 1.2 – Guide d'utilisation*. Québec.

Brown, R. D. (2010). Analysis of snow cover variability and change in Québec 1948-2005. *Hydrological processes, 24*, 1929-1954.

Buttle, J. M., Allen, D. M., Caissie, D., Davison, B., Hayashi, M., Peters, D. L., . . . Whitfield, P. H. (2016). Flood processes in Canada: Regional and special aspects. *Canadian Water Resources Journal, 41*, 7-30.

Coles, A. E., Appels, W. M., McConkey, B. G., & McDonnelll, J. J. (2016). The hierarchy of controls on snowmelt-runoff generation over seasonally-frozen hillslopes. *Hydrology and earth system, 2016*, 1-27.

Curry, C. L., & Zwiers, F. W. (2017). Examining controls on peak annual streamflow and floods in the Fraser River Basin of British Columbia. *hydrology and earth system, 22*, 2285-2309.

Dyer, J. (2008). Snow depth and streamflow relationships in large North American watersheds. *Journal of geophysical research, 113*.

Ellis, C., Pomeroy, J. W., Essery, R. L. H., & Link, T. E. (2011). Effects of needleleaf forest cover on radiation and snowmelt dynamics in the Canadian Rocky Mountains. *Canadian Journal of Forest Research 41*, 608-620.

Fang, X., & Pomeroy, J. W. (2016). Impact of antecedent conditions on simulations of a flood in amountain headwater basin. *Hydrological process, 30*, 2754-2772.

Fortin, J.-P., Turcotte, R., Massicotte, S., Moussa, R., Fitzback, J., & Villeneuve, J.-P. (2001). Distributed watershed model compatible with remote Sensing and gis data. I: description of model. *Journal of hydrologic engineering, 6*(2), 1084-0699.

Foster, K., Uvo, C. B., & Olsson, J. (2018). The development and evaluation of a hydrological seasonal forecast system prototype for predicting spring flood volumes in Swedish rivers. *Hydrology and Earth System Sciences, 22*, 2953-2970.

Garvelmann, J., Pohl, S., & Weilerl, M. (2015). Spatio-temporal controls of snowmelt and runoff generation during rain-on-snow events in a mid-latitude mountain catchment. *Hydrological process, 29*, 3649-3664.

Koster, R. D., Mahanama, S. P. P., Livneh, B., Lettenmaier, D. P., & Reichlel, R. H. (2010). Skill in streamflow forecasts derived from large-scale estimates of soil moisture and snow. *Nature geoscience, 22*, 872-882.

Li, H., Luo, L., Wood, E. F., & Schaake, J. (2009). The role of initial conditions and forcing uncertainties in seasonal hydrologic forecasting. *Journal of geophysical research, 114*, 1-10.

Mahanama, S., Livneh, B., Koster, R., Lettenmaier, D., & Reichle, R. (2012). Soil Moisture, Snow, and Seasonal Streamflow Forecasts in the United States. *Journal of hydrometeorology, 13*, 189-203.

Mazouz, R., Assani, A. A., & Rodríguez, M. A. (2013). Application of redundancy analysis to hydroclimatology: A case study of spring heavy floods in southern Québec (Canada). *Journal of Hydrology, 496*, 187-194.

Mccabe, G. J., Clark, M. P., & Hay, a. E. (2007). rain-on-snow events in the western united states. *American meteorological soceity 88*, 319-328.

Musselman, K. N., Clark, M. P., Liu, C., Ikeda, K., & Rasmussen, R. (2017). Slower snowmelt in a warmer world. *Nature Climate Change, 7*, 214-219.

Nied, M., Hundecha, Y., & Merz, B. (2013). Flood-initiating catchment conditions: a spatio-temporal analysis of large-scale soil moisture patterns in the Elbe River basin. *Hydrology and earth system, 17*, 1401-1414.

Nied, M., Pardowitz, T., Nissen, K., Ulbrich, U., Hundecha, Y., & Merz, B. (2014). On the relationship between hydro-meteorological patterns and flood types. *Journal of hydrology, 519*, 3249-3262.

Pomeroy, J. W., Fang, X., & Marks, D. G. (2016). The cold rain-on-snow event of June 2013 in the Canadian Rockies – characteristics and diagnosis. *Hydrological processes, 30*, 2899-2914.

Saad, C., Adlouni, S. E., St-Hilaire, A., & Gachon, P. (2015). A nested multivariate copula approach to hydrometeorological simulations of spring floods: the case of the Richelieu River (Quebec, Canada) record flood. *Stoch Environ Res Risk Assess 2015*, 275-294.

Saint-Laurent, D., Mesfioui, M., & Evin, G. (2009). Hydroclimatic Variability and Relation with Flood Events (Southern Québec, Canada). *Water Resources 36*(1), 43-56.

Sena, N., Chokmani, K., Gloaguen, E., & Bernier, M. (2016). Analyse multi échelles de la variabilité spatiale de l'équivalent en eau de la neige (EEN) sur le territoire de l'Est du Canada. *Hydrological Sciences Journal*, 1-16.

Sui, J., & Koehler, G. (2001). rain on snow induced flood events in Southern Germany *Journal of hydrology, 252*, 205-220.

Teufel, B., Sushama, L., Huziy, O., Diro, G. T., Jeong, D. I., Winger, K., . . . Nguyen, V. T. V. (2018). Investigation of the mechanisms leading to the 2017 Montreal flood. *Climat dynamics*, 1-14.

Turcotte, R., Filion, T.-C. F., Lacombe, P., Fortin, V., Roy, A., & Royer, A. (2010). Simulation hydrologique des derniers jours de la crue de printemps : le problème de la neige manquante. *Hydrological Sciences Journal, 55*(6), 872-882.

Valéry, A. (2010). *Modélisation précipitations – débit sous influence nivale : Elaboration d'un module neige et évaluation sur 380 bassins versants.* Thèse de doctorat, AgroParisTech, Paris.

Valéry, A., Andréassian, V., & Perrin, C. (2014b). 'As simple as possible but not simpler': What is useful in a temperature-based snow-accounting routine? Part 2 – Sensitivity analysis of the Cemaneige snow accounting routine on 380 catchments. *Journal of Hydrology, 517*, 1176-1187.

Wayand, N. E., Lundquist, J. D., & Clark, M. P. (2015). Modeling the influence of hypsometry, vegetation, and storm energy on snowmelt contributions to basins during rain-on-snow floods. *Water ressources research, 51*, 8551-8569.

Webb, R. W., Fassnacht, S. R., & Gooseff, M. N. (2018). Hydrologic flow path development varies by aspect during spring snowmelt in complex subalpine terrain. *The Cryosphere, 12*, 287-300.

Wever, N., Comola, F., Bavay, M., & Lehning, M. (2017). Influence of snow surface processes on soil moisture dynamics and streamflow generation in alpine catchments. *Hydrology and earth system sciences, 21*, 4053-4071.

CHAPITRE IV

CONCLUSION GÉNÉRALE

L'objectif principal de ce projet était d'étudier les caractéristiques hydrométéorologiques des crues printanières au Québec à l'aide d'un modèle hydrologique simplifié (modèle GR4J) et un modèle de fonte à base de degré/jours (modèle Cemaneige) pour la compréhension des facteurs qui préconditionnent les crues printanières au Québec. Les paramètres du modèle GR4J et les paramètres de Cemaneige liés à la neige ont été calés et validés sur 12 bassins des affluents naturels du fleuve Saint-Laurent au Québec dans le but d'améliorer la simulation du manteau nival avec quatre stratégies de calibration. La multiplicité des jeux optimums qui donnent la même performance équifinalité et la faible identifiabilité de certains paramètres sont les principaux problèmes rencontrés pour identifier le jeu de paramètres optimal dans un modèle hydrologique. La simulation du stock de neige est aussi un autre enjeu rencontré lors de l'utilisation de ces modèles simplifiés.

La contribution de la première partie de cette étude (chapitre II) est d'étudier l'apport de l'utilisation des points de mesure *in situ* au Québec dans la calibration sur la performance globale, la simulation de couvert nival et l'équifinalité des paramètres. Nos principaux résultats montrent que :

1) La calibration sur les débits observés seulement a donné une bonne simulation de débit, mais une mauvaise simulation de couvert nival dans les deux premières méthodes où la calibration est faite seulement avec le débit observé. La calibration du modèle de fonte séparément dans la troisième méthode a montré un surajustement du modèle à la simulation de l'ÉEN et une dégradation significative globale au niveau de la simulation des débits par rapport aux deux autres méthodes utilisant seulement les débits observés. Par contre, la calibration multi-objectif par AMALGAM sur les observations

des débits et d'ÉEN a donné la meilleure simulation de couvert nival et de débit. Cette amélioration de la simulation de l'ÉEN sans dégrader la simulation des débits montre l'importance d'inclure les points de mesure *in situ* au Québec pour améliorer la simulation de la neige dans un modèle hydrologique conceptuel.

2) L'incertitude structurelle de modèles GR4J due à la forte interaction et la faible identifiabilité des paramètres est la principale source d'équifinalité des paramètres. En effet, l'étude de sensibilité effectuée dans le cadre de cette étude a montré que le modèle est le plus sensible au coefficient d'échange (x2) (échange avec la nappe) pour ajuster le bilan en eau. Le nombre de jeux équifinaux et le test d'identifiabilité dynamique montrent également la faible identifiabilité de certains paramètres. La corrélation entre les jeux équifinaux démontre la compensation entre certains paramètres du modèle GR4J.

3) La calibration multi-objectif a montré aussi sa capacité à réduire la dispersion des paramètres équifinaux.

4) Les résultats ont également montré que les incertitudes qui peuvent être induites en utilisant le jeu de paramètres optimal plutôt que les jeux de paramètres équifinaux pour la détection de l'évolution du débit maximum printanier dans un contexte des changements climatiques dans les bassins dominés par la neige ne sont pas négligeables, d'où l'importance de prendre en compte ce type d'incertitude dans les études d'impact des changements climatiques.

La conclusion de cette première partie est que la structure grossière des modèles conceptuels, la faible identifiabilité des paramètres et l'absence de données complémentaires ouvrent la porte au surajustement des modèles. L'ajout d'information complémentaire (les points de neige) aux débits pour mieux contraindre ces paramètres semble être la meilleure façon pour simuler tous les processus correctement et réduire la dispersion des paramètres.

L'objectif de la deuxième partie était de déterminer les principaux facteurs qui contrôlent la variabilité interannuelle des pics de crue printanière, ainsi leur date d'occurrence. Les principaux résultats montrent que globalement, le classement des facteurs de préconditionnement obtenus par la régression linéaire et qui expliquent la variabilité interannuelle de la magnitude des crues printanières à travers les douze bassins est le suivant : (i) l'intensité de fonte (moyenne et maximale), (iii) la somme de la fonte, (iv) la somme de la pluie, (v) le pic du SWE (Gmax) et (vi) de l'humidité du sol. La date d'occurrence est contrôlée dans la plupart des bassins par la somme et l'intensité de pluie pré-crue et la date d'occurrence étant plus hâtive lorsque les pluies sont plus abondantes et intenses. Dans les bassins les plus au nord, dominés par la neige et avec un régime hydrologique nival, c'est la pluie qui contrôle le plus les variations interannuelles des pics de débit, tandis que dans les bassins plus pluvieux du sud, la variabilité de couvert nival contrôle davantage cette variabilité. Il semble également que pour les bassins plus boisés, la fonte est naturellement plus graduelle, de sorte que les variations du stock de neige ont moins d'influence que la pluie sur la variabilité de la magnitude des crues. En revanche, pour les bassins plus agricoles qui ont une fonte naturellement plus rapide c'est la variation du stock de neige qui a une plus grande influence sur la magnitude des crues.

RÉFÉRENCES BIBLIOGRAPHIQUES

Adamowski, K. (2000). Regional analysis of annual maximum and partial duration flood data by non-parametric L-moment methods. *Journal of Hydrology, 299*, 219-231.

Assani, A., Landry, R., & Laurencelle, M. (2012). Comparison of interannual variability modes and trends of seasonal precipitation and streamflow in southern Quebec (Canada). *River Research And Applications, 28*, 1740-1752.

Brown, R. D. (2010). Analysis of snow cover variability and change in Québec 1948–2005. *Hydrological processes, 24*, 1929-1954.

Buttle, J. M., Allen, D. M., Caissie, D., Davison, B., Hayashi, M., Peters, D. L., . . . Whitfield, P. H. (2016). Flood processes in Canada: Regional and special aspects. Canadian Water Resources Journal, 1918-1817.

Buttle, J. M., Allen, D. M., Caissie, D., Davison, B., Hayashi, M., Peters, D. L., . . . Whitfield, P. H. (2016). Flood processes in Canada: Regional and special aspects. *Canadian Water Resources Journal, 41*, 7-30.

Troin, M., Arsenault, R., & Brissette, F. (2015). Performance and Uncertainty Evaluation of Snow Models on Snowmelt Flow Simulations over a Nordic Catchment (Mistassibi, Canada). *Hydrology 2*, 289-317.

Turcotte, R. (2010). *Éléments du calage et de l'implantation d'un modèle hydrologique dans une perspective d'utilisation opérationnelle en prévision hydrologique.* Thèse de doctorat, Université du Québec.

Valéry, A., Andréassian, V., & Perrin, C. (2014a). 'As simple as possible but not simpler': What is useful in a temperature-based snow-accounting routine? Part 1 – Comparison of six snow accounting routines on 380 catchments. *Journal of Hydrology, 514*, 1166-1175.

Valéry, A., Andréassian, V., & Perrin, C. (2014b). 'As simple as possible but not simpler': What is useful in a temperature-based snow-accounting routine? Part 2 – Sensitivity analysis of the Cemaneige snow accounting routine on 380 catchments. *Journal of Hydrology, 517*.